



OPEN ACCESS

Edited by:

Cai-Zhong Jiang,
USDA-ARS, United States

Reviewed by:

Carlos H. Crisosto,
University of California, Davis,
United States
Macarena Faruqh,
University of Maryland, College Park,
United States

***Correspondence:**

Fumio Fukuda
ffukuda@okayama-u.ac.jp
Koichiro Ushijima
ushijima@cc.okayama-u.ac.jp

† These authors
have contributed equally to this work

‡ Present address:

Yosuke Fukamatsu,
Research Institute for Biological
Sciences, Okayama Prefectural
Technology Center for Agriculture,
Forestry, and Fisheries, Okayama,
Japan

Specialty section:

This article was submitted to
Crop and Product Physiology,
a section of the journal
Frontiers in Plant Science

Received: 23 April 2020

Accepted: 28 October 2020

Published: 26 November 2020

Citation:

Nakano R, Kawai T, Fukamatsu Y,
Akita K, Watanabe S, Asano T,
Takata D, Sato M, Fukuda F and
Ushijima K (2020) Postharvest
Properties of Ultra-Late Maturing
Peach Cultivars and Their Attributions
to Melting Flesh (*M*) Locus:
Re-evaluation of *M* Locus
in Association With Flesh Texture.
Front. Plant Sci. 11:554158.
doi: 10.3389/fpls.2020.554158

Postharvest Properties of Ultra-Late Maturing Peach Cultivars and Their Attributions to *Melting Flesh* (*M*) Locus: Re-evaluation of *M* Locus in Association With Flesh Texture

Ryohei Nakano^{1†}, Takashi Kawai^{2†}, Yosuke Fukamatsu^{2‡}, Kagari Akita², Sakine Watanabe², Takahiro Asano², Daisuke Takata³, Mamoru Sato³, Fumio Fukuda^{2*} and Koichiro Ushijima^{2*}

¹ Experimental Farm of Graduate School of Agriculture, Kyoto University, Kizugawa, Kyoto, Japan, ² Graduate School of Environmental and Life Science, Okayama University, Okayama, Japan, ³ Faculty of Food and Agricultural Sciences, Fukushima University, Fukushima, Japan

The postharvest properties of two ultra-late maturing peach cultivars, “Tobihaku” (TH) and “Daijimitsuto” (DJ), were investigated. Fruit were harvested at commercial maturity and held at 25°C. TH exhibited the characteristics of normal melting flesh (MF) peach, including rapid fruit softening associated with appropriate level of endogenous ethylene production. In contrast, DJ did not soften at all during 3 weeks experimental period even though considerable ethylene production was observed. Fruit of TH and DJ were treated with 5,000 ppm of propylene, an ethylene analog, continuously for 7 days. TH softened rapidly whereas DJ maintained high flesh firmness in spite of an increase in endogenous ethylene production, suggesting that DJ but not TH lacked the ability to be softened in response to endogenous and exogenous ethylene/propylene. DNA-seq analysis showed that tandem endo-polygalacturonase (*endoPG*) genes located at *melting flesh* (*M*) locus, *Pp-endoPGM* (*PGM*), and *Pp-endoPGF* (*PGF*), were deleted in DJ. The *endoPG* genes at *M* locus are known to control flesh texture of peach fruit, and it was suggested that the non-softening property of DJ is due to the lack of *endoPG* genes. On the other hand, TH possessed an unidentified *M* haplotype that is involved in determination of MF phenotype. Structural identification of the unknown *M* haplotype, designated as *M*⁰, through comparison with previously reported *M* haplotypes revealed distinct differences between *PGM* on *M*⁰ haplotype (*PGM-M*⁰) and *PGM* on other haplotypes (*PGM-M*¹). Peach *M* haplotypes were classified into four main haplotypes: *M*⁰ with *PGM-M*⁰; *M*¹ with both *PGM-M*¹ and *PGF*; *M*² with *PGM-M*¹; and *M*³ lacking both *PGM* and *PGF*. Re-evaluation of *M* locus in association with MF/non-melting flesh (NMF) phenotypes in more than 400 accessions by using whole genome shotgun sequencing data on database and/or by PCR genotyping demonstrated that *M*⁰ haplotype was the common haplotype in MF accessions, and *M*⁰ and *M*¹ haplotypes

were dominant over M^2 and M^3 haplotypes and co-dominantly determined the MF trait. It was also assumed on the basis of structural comparison of M haplotypes among *Prunus* species that the ancestral haplotype of M^0 diverged from those of the other haplotypes before the speciation of *Prunus persica*.

Keywords: fruit, softening, ethylene, *Prunus persica*, melting flesh locus, endoPG, postharvest

INTRODUCTION

Fruit firmness is an important quality that influences consumer preference, damage during distribution, and shelf life. Studies associated with the decrease in fruit firmness after harvest have been conducted with an eye toward reducing distribution loss and prolonging shelf life and thus, supplying high-quality fruit to consumers (Nimmakayala et al., 2016; Moggia et al., 2017; Tucker et al., 2017; Fernandez et al., 2018; Liu et al., 2018; Carrasco-Valenzuela et al., 2019). Fruit can be classified as climacteric or non-climacteric depending on their respiration and ethylene production patterns during ripening (Biale and Young, 1981). In climacteric fruit, ethylene is acknowledged to play an important role in controlling ripening- and senescence-related phenomena including fruit softening, due to the fact that massive ethylene production commences at the onset of ripening; exogenously applied ethylene and/or ethylene analog, propylene, induces ripening and senescence; ethylene inhibitors retard the progress of fruit ripening and senescence; and mutants and transgenic lines defective in ethylene production ability exhibit suppressed fruit ripening, especially softening (Gapper et al., 2013; Minas et al., 2015; Tucker et al., 2017).

Peach [*Prunus persica* (L.) Batsch] is generally known to belong to the climacteric type and to exhibit dramatic increases in respiration and ethylene production during ripening (Tonutti et al., 1991). In melting flesh (MF) peaches, the increased ethylene stimulates fruit softening principally through cell wall modification (Brummell et al., 2004; Hayama et al., 2006, 2008; Liu et al., 2018). MF peaches are highly perishable, softening rapidly after harvest. The increasing interest in improving peach shelf life has sparked investigations and resulted in findings of peach strains with long shelf lives. Those studies have demonstrated phenotypic variability associated with fruit softening and identified the possible causal genes for peach shelf life, as described below.

Intensively studied peaches that have long shelf lives are the stony-hard (SH) and slow-ripening (SR) peaches (Brecht and Kader, 1984; Haji et al., 2005; Bassi and Monet, 2008). The SH is determined by *Hdhd* gene and fruit with SH flesh bear the *hdhd* genotype (Haji et al., 2005). SH peaches are characterized by the absence of ethylene production and high firmness during postharvest storage, which are caused by the reduced expression of ethylene biosynthesis related gene *PpACS1* encoding 1-aminocyclopropane-1-carboxylic acid

synthase (Tatsuki et al., 2006). *YUCCA* flavin mono-oxygenase gene *PpYUC11*, which is involved in the auxin biosynthesis pathway, has been proposed as a candidate for causal gene for this phenotype (Pan et al., 2015; Tatsuki et al., 2018). SR peaches are known to show delayed maturation on the tree, thereby resulting in late harvest. In SR peaches harvested earlier than the optimum harvest date, flesh firmness decreased slowly (Brecht and Kader, 1984). Its genetic base was characterized and a deletion mutation in a gene encoding the NAC transcription factor was reported to be responsible for the SR phenotype (Eduardo et al., 2015; Nuñez-Lillo et al., 2015; Meneses et al., 2016).

Another peach strain that shows high flesh firmness during postharvest ripening is non-melting flesh (NMF) peaches (Fishman et al., 1993; Yoshioka et al., 2011). Whereas MF peaches soften dramatically and bear melting texture during the final stage of ripening called “melting phase,” NMF fruit appear to lack this “melting phase” of softening and remain relatively firm during ripening not only on the tree and but also after harvest (Fishman et al., 1993; Yoshioka et al., 2011). The MF/NMF phenotypes segregate as a single locus (M) that is linked tightly to the stone adhesion locus (Bailey and French, 1949; Monet, 1989). MF is dominant over NMF and the recessive allele determines the NMF character (Bailey and French, 1949; Monet, 1989). In NMF peaches, solubilization of cell wall pectin and enzymatic activity and protein accumulation of endo-polygalacturonase (endoPG), a pectin hydrolase, are markedly reduced compared with MF peaches (Pressey and Avants, 1978; Fishman et al., 1993; Lester et al., 1996; Yoshioka et al., 2011). Studies aimed at demonstrating *endoPG(s)* as a candidate gene for M locus have shown suppressed or undetectable expression of *endoPG(s)* in NMF peaches and polymorphisms in *endoPG* genes coinciding with MF/NMF phenotypes (Lester et al., 1994, 1996; Callahan et al., 2004; Peace et al., 2005, 2007; Morgutti et al., 2006, 2017; Gu et al., 2016). M locus is located at 3.5 cM interval on the bottom of linkage group 4 of the peach map, the position within which a genomic region with clusters of *endoPG* genes exists (Cao et al., 2016; Gu et al., 2016). Two tandem *endoPG* genes in that region, *Pp-endoPGM* (*PGM*) and *Pp-endoPGF* (*PGF*), corresponding to sequences *Prupe.4G262200* in v2.0 of peach genome (*ppa006857m* in v1.0) and *Prupe.4G261900* (*ppa006839m* in v1.0), respectively, were found to be responsible for determining the MF/NMF phenotypes (Gu et al., 2016). Gu et al. (2016) proposed a scenario where M locus has three allelic copy number variants of *endoPG* genes designated by H_1 (possessing *PGF* and *PGM*), H_2 (only *PGM*), and H_3 (*null*). Accessions harboring either H_1 and/or H_2 haplotype (H_1H_1 , H_1H_2 , H_1H_3 , H_2H_2 , and H_2H_3) exhibit MF phenotype whereas those harboring homozygous recessive H_3 (H_3H_3) show NMF

Abbreviations: M locus, Melting flesh locus; MF, melting flesh; NMF, non-melting flesh; SH, stony-hard; SR, slow-ripening; SSC, soluble solids content; endo-PG, endo-polygalacturonase; NADH, nicotinamide adenine dinucleotide dehydrogenase; SRA, sequence read archive; WGS, whole genome shotgun sequencing; SNP, single nucleotide polymorphism; indel, insertion/deletion.

phenotype (Gu et al., 2016). It was also speculated that H₂ is the ancestral haplotype whereas H₁ and H₃ haplotypes are two variants due to the duplication and deletion of *PGM*, respectively, (Gu et al., 2016). However, research on different NMF peach germplasms suggested that mutations in *endoPG* gene(s) could be of more than one type arising from more than one source (Lester et al., 1996; Callahan et al., 2004; Peace et al., 2005; Morgutti et al., 2006, 2017) and some NMF accessions seemed to be incompatible with the model proposed by Gu et al. (2016). Much more comprehensive evaluation of *M* locus in association with flesh textural traits is required. Pursuing *M* locus evolution with much broader genetic resources covering *Prunus* species is also necessary for precise judgment.

Peach is known to have high diversity with regard to not only flesh texture but also fruit maturation date (Elsadr et al., 2019). In Japan, MF peaches reaching maturation stage in early July through September are mainly produced. Recently, because of the increasing demand for fresh peach in late autumn, ultra-late maturing cultivars whose optimum harvest dates are October and November are gathering the attention of growers. However, the postharvest properties of some of these rare cultivars have not yet been characterized.

In this study, first, two postharvest properties, namely, ethylene production and fruit softening, of two extremely late harvest cultivars, “Tobihaku” (TH) and “Daijumitsuto” (DJ), were investigated. It was revealed that TH showed normal MF peach ripening properties, whereas DJ possessed unique properties in that the fruit did not soften at all in spite of significant endogenous ethylene production and exogenous propylene treatment. Second, DNA-seq analysis of these cultivars demonstrated that DJ was a homozygote of an allele lacking *PGM* and *PGF* at *M* locus, whereas TH possessed a previously structurally unidentified haplotype that contained one *endoPG*. Third, accessing database sequences at *M* locus in more than 400 peach accessions and *Prunus* species indicated that the newly identified haplotype was an important allele that distributed widely within MF accessions, determined MF phenotype, and seemed to have been diverse from the other haplotypes before the speciation of *P. persica*. The scenario is discussed in which not three but four allelic variants at *M* locus are associated with the flesh texture and the newly identified haplotype is one of the two dominant determinants of MF texture.

MATERIALS AND METHODS

Plant Materials

Ultra-late maturing peach (*Prunus persica*) cultivars “Tobihaku” (TH) and “Daijumitsuto” (DJ), whose genetic backgrounds are unknown, were examined. TH fruit were harvested on November 7, 2018, the commercial harvest date, from two trees grown in a commercial orchard in Okayama Prefecture located in southwestern Japan. DJ fruit were harvested on October 12, 2018, the commercial harvest date, from two trees grown in the Research Farm of Okayama University. For each cultivar, 26 fruit without any disease and injuries were selected and used for investigation described below. As

regards DJ, 16 fruit from a different production area, namely, Fukushima Prefecture, which is located in northeastern Japan, were harvested on October 22, 2018, the commercial harvest date, and 12 fruit without any disease and injuries after transfer to Okayama were used to investigate the effects of growing conditions and harvest maturity. Climate conditions in the peach production areas, which were obtained from the website of the Japan Meteorological Agency¹, are listed in **Supplementary Table S1**. Regardless of cultivar or growing area, fruit were grown under suitable climate conditions for peach production by skilled growers using conventional growing techniques in Japan, including fruit thinning and bagging by the end of June. The fruit were harvested on the basis of skilled growers’ visual evaluation using de-greening of fruit ground color as harvest index. It is equivalent to color chip No. 3 (color meter score of L: 76.8, a*: −8.16, b*: 29.7) of de-greening harvest index reported in Yamazaki and Suzuki (1980). After harvest, 16 out of the 26 fruit of TH and DJ harvested from Okayama Prefecture were ripened at 25°C for 3 weeks and ethylene production rate, flesh firmness, soluble solids content (SSC), and juice pH were measured on days 0, 7, 14, and 21 at 25°C. DJ fruit harvested from Fukushima Prefecture were packed carefully in a corrugated cardboard box and transported by vehicle at ambient temperature to Okayama University 2 days after harvest, where 12 fruit without any disease and injuries were ripened at 25°C.

Propylene Treatment

Ten out of 26 fruit of TH and DJ harvested from Okayama Prefecture were used for experiment with continuous propylene treatment. Six fruits per each cultivar, excluding those used for measurement of values at day 0, were treated with 5,000 ppm of propylene, an ethylene analog, continuously for 7 days at 25°C, as described previously (McMurchie et al., 1972; Hiwasa et al., 2004). Ethylene production rates and flesh firmness were measured on treatment days 0, 3, and 7.

Measurement of Ethylene Production Rate, Flesh Firmness, SSC, and Juice pH

Ethylene production rate, flesh firmness, SSC, and juice pH were measured as described previously (Kawai et al., 2018; Nakano et al., 2018). For the measurement of ethylene production rate, individual fruit were incubated in a 1.3 L plastic container at room temperature for 30 min. Headspace gas withdrawn from the container was injected into a gas chromatograph (GC8 CMPF; Shimadzu, Kyoto, Japan) equipped with a flame ionization detector (set at 200°C) and an activated alumina column (ϕ 4 mm × 1 m) set at 80°C. For flesh firmness, the cheek parts of each fruit were cut and peeled, and flesh penetration force was measured using a rheometer (FUDOH RTC Rheometer; RHEOTECH, Tokyo, Japan) with a 3-mm-diameter cylindrical plunger and expressed in Newton per plunger area (N/mm²). The relationships between the flesh penetration force measured by this system and fruit maturity indexes are listed in **Supplementary Table S2**. SSC and juice pH in the cheek parts of each fruit were measured with a

¹<http://www.jma.go.jp/jma/index.html>

refractometer (PR-1; Atago, Tokyo, Japan) and a pH meter (B-712; HORIBA, Kyoto, Japan), respectively.

Statistical Analysis

Three to four fruit were used as biological replicates at each measurement point. In order to evaluate postharvest changing patterns in flesh firmness and ethylene production in different cultivars or production areas under the condition with and without propylene, Tukey's multiple comparison test was conducted after one-way ANOVA. The different letters shown in each figure indicate significant differences among measurement days by Tukey's test ($p < 0.05$).

Mapping WGS Data and Variant Calling

Genomic DNA was isolated from the leaves of DJ, TH, and "Benihakuto" (BH) by Nucleon PhytoPure (Cytiva). DNA-seq analysis was performed by Novogen and 9G data of PE150 reads, corresponding to approx. 30 times coverage, were obtained. We further searched SRA (Sequence Read Archive) database to obtain whole genome shotgun sequencing (WGS) data for doubled haploid "Lovell" (dhLL), "Dr. Davis" (DD), and "Big Top" (BT). Illumina WGS reads were mapped to peach reference genome (ver. 2.0) (Verde et al., 2017) by CLC Genomics Workbench or minimap2 (Li, 2018). SNP, indel, and structural variants were called by CLC Genomics Workbench.

De novo Assembly and Structural Comparison

DNA-seq analysis of BH was further performed by Macrogen to obtain 46G data of PE150 reads, which correspond to approx. 170 times coverage of *P. persica* genome. Illumina reads were assembled by ABySS 2.0 (Jackman et al., 2017). Contigs encompassing *M* locus were detected by Blastn analysis using *PG1*, *PG2*, *PGM/F*, *NADH*, and *F-box* genes, which were located in the *M* locus region, as query. M^0 and M^1 haplotype sequences (see section "Results") were compared by nucmer (Kurtz et al., 2004) and their relationship was drawn by Circos². We generated new reference sequence set "PpREF20 + M0," in which the M^0 haplotype sequence was added to *P. persica* reference genome. Illumina short reads of DJ, TH, BH, dhLL, DD, and BT were mapped to PpREF20 + M0 by minimap2. Coverage was analyzed from BAM file by samtools and drawn by Circos.

Genotyping by PCR

Genomic DNA was extracted from leaves of peach accessions. Genotyping by PCR was conducted with six sets of primers described in **Supplementary Table S3**. PCR was performed with BIOTAQ DNA Polymerase (Bioline, United Kingdom) using the following program: 30–35 cycles at 95°C for 20 s, annealing for 15 s, and extension at 72°C an initial denaturation at 95°C for 3 min, and a final extension at 72°C for 7 min. Annealing temperature and extension time are described under "PCR conditions" in **Supplementary Table S3**. PGM/F products were separated on a 15% acrylamide gel and others were separated on

an agarose gel. PCR products were stained with UltraPower DNA Safedye (Gellex International Co., Ltd., Japan).

RESULTS

Fruit Ripening Characteristics of Two Ultra-Late Maturing Cultivars

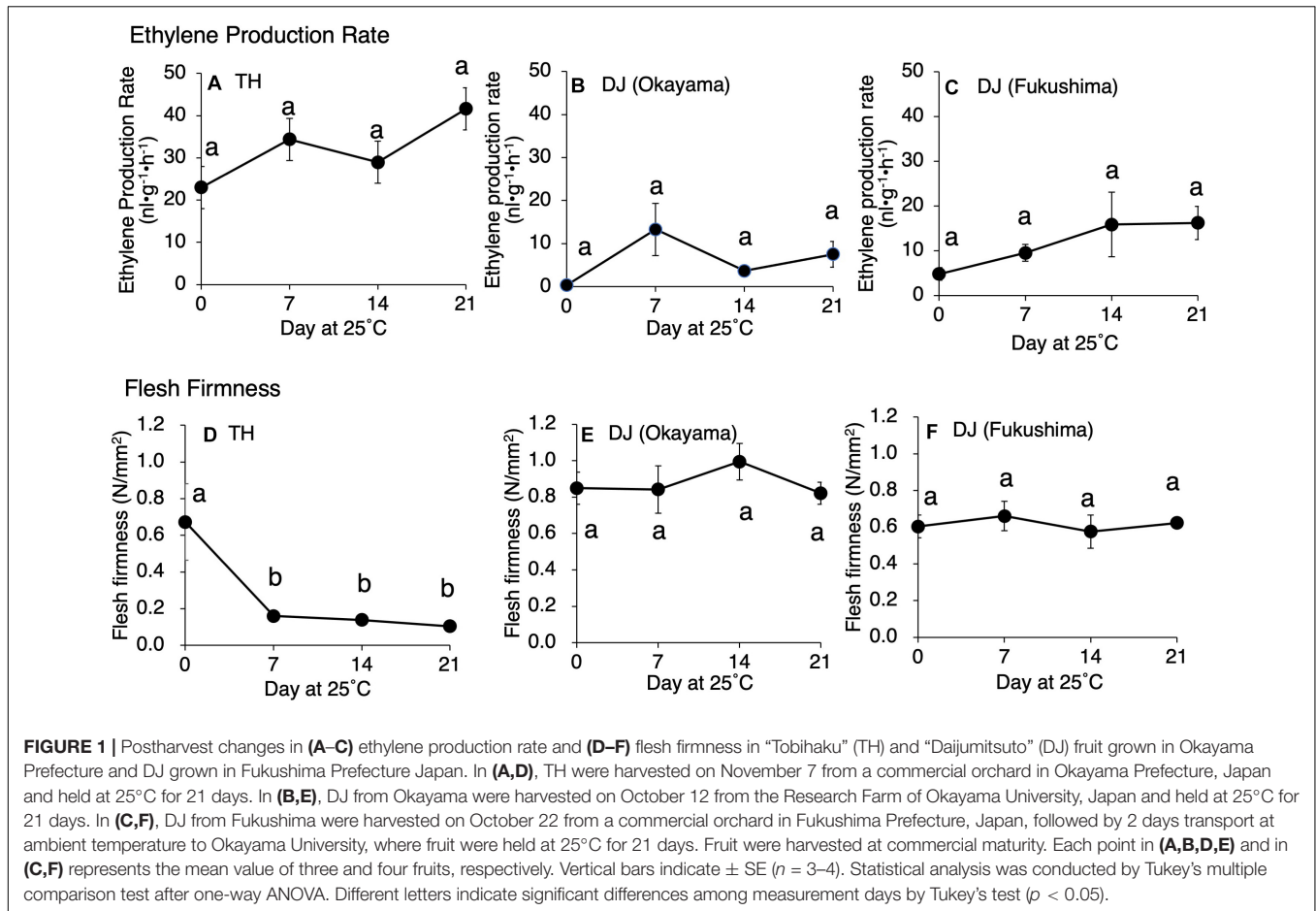
Postharvest changes in ethylene production rate, flesh firmness, SSC, and juice pH were investigated in two ultra-late maturing peach cultivars, TH and DJ. In TH, as much as 22 $\text{nl}\cdot\text{g}^{-1}\cdot\text{h}^{-1}$ of ethylene was produced at harvest and the amount increased gradually during storage at 25°C (**Figure 1A**). Flesh firmness was 0.7 N/mm^2 at harvest but decreased dramatically to less than 0.2 N/mm^2 by day 7 at 25°C (**Figure 1D**). Thereafter, the decrease became slight until the last day of experiment (day 21). SSC and juice pH did not change remarkably during storage (**Supplementary Figure S1**). In DJ harvested from the Research Farm of Okayama University on October 12, ethylene production rate was almost negligible at harvest. Thereafter, ethylene production rate increased and peaked on day 7, reaching more than 10 $\text{nl}\cdot\text{g}^{-1}\cdot\text{h}^{-1}$ (**Figure 1B**). Flesh firmness was around 0.85 N/mm^2 at harvest (**Figure 1E**). In spite of considerable ethylene production, flesh firmness showed no significant decrease during storage at 25°C and was almost unchanged until the last day of experiment (day 21). SSC slightly increased during storage, reaching a peak of 18 °Brix on day 14, and juice pH was maintained at around pH 4.0 during storage (**Supplementary Figure S1**).

To confirm that the unique characteristics of DJ were not due to climatic effects and/or misestimated harvest maturity, DJ fruit harvested from a different production area were investigated. In the case of DJ harvested from a commercial orchard in Fukushima Prefecture on October 22, fruit delivered to Okayama University two days after harvest had an ethylene production rate of as high as 5.2 $\text{nl}\cdot\text{g}^{-1}\cdot\text{h}^{-1}$ and flesh firmness of 0.6 N/mm^2 (**Figures 1C,F**). Substantially high level of ethylene production was maintained during storage at 25°C, scoring 16 $\text{nl}\cdot\text{g}^{-1}\cdot\text{h}^{-1}$ on day 21. On the other hand, flesh firmness did not change significantly during storage; flesh firmness on day 21 was almost the same as that at harvest. SSC and juice pH did not change remarkably during storage (**Supplementary Figure S1**). **Figure 2** shows DJ fruit on day 14. The external appearance showed no significant deterioration; however, the longitudinal sections showed flesh browning and slight flesh breakdown around the stones.

Different Responses to Exogenous Propylene Treatment of TH and DJ

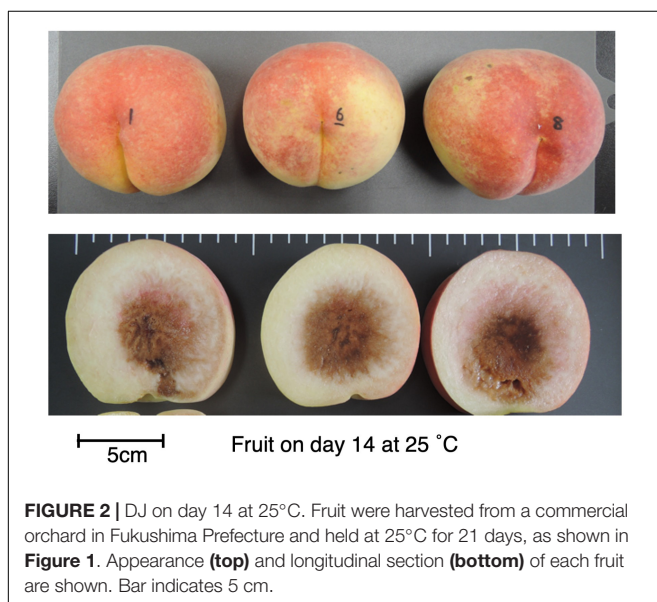
Although ethylene production rate during storage was higher in TH than DJ, generally speaking, the amount of ethylene produced in DJ is sufficient to induce physiological effects on fruit ripening including flesh softening (Mathooko et al., 2001; Hiwasa et al., 2004; Nishiyama et al., 2007; Hayama et al., 2008; Liu et al., 2018). In order to confirm that the non-softening characteristic of DJ is not due to the low ethylene production rate of this

²<http://circos.ca>



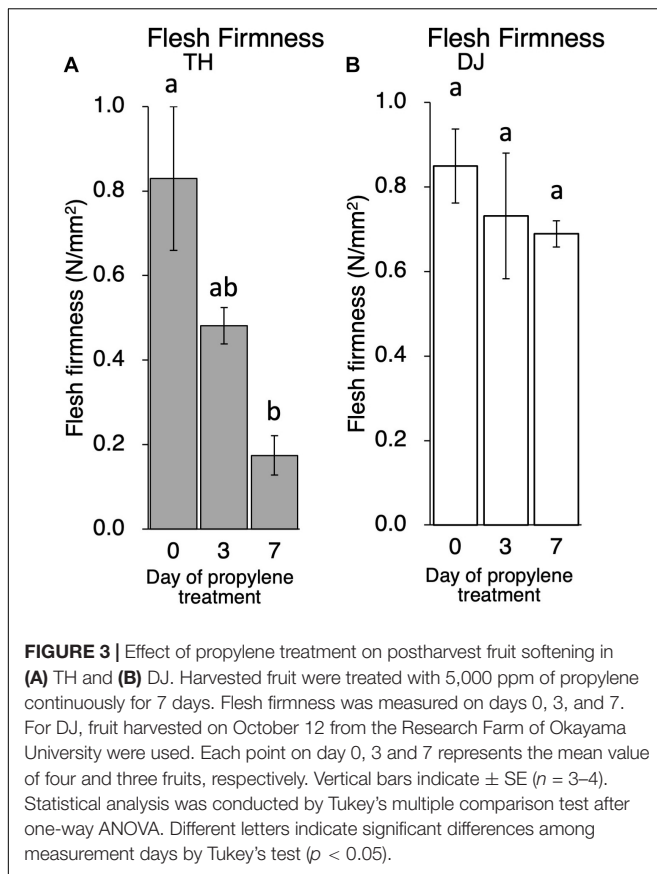
cultivar, TH and DJ were treated with 5,000 ppm of propylene, an ethylene analog, continuously for 7 days. This concentration of propylene is equivalent to 50 ppm of ethylene and is sufficient

to induce ethylene response in climacteric fruits (Burg and Burg, 1967; McMurchie et al., 1972). Ethylene production rates of TH and DJ were increased rapidly by the propylene treatment, reaching 45 and 22 $\text{nl}\cdot\text{g}^{-1}\cdot\text{h}^{-1}$ on day 3 of treatment, respectively (Supplementary Figure S2). Flesh firmness of TH decreased rapidly whereas that of DJ decreased slightly, and high firmness was maintained in DJ even after 7 days of continuous propylene treatment (Figure 3). These results suggest that regardless of the differences in the ethylene production rate, DJ lacked the ability to be softened in response to ethylene.



Structural Features of *M* Locus in DJ and TH and an Unidentified Haplotype in TH

M locus is involved in the regulation of peach flesh texture (Bailey and French, 1949; Monet, 1989; Bassi and Monet, 2008). Four polygalacturonase genes, *PG1*, *PG2*, *PGM*, and *PGF*; three *NADHs*; and one *F-box* gene were annotated in the *M* locus region of peach reference genome (Figure 4A). Gu et al. (2016) walked the chromosome of three accessions by using PCR based on sequence information of reference genome, and proposed three haplotypes, *H*₁, *H*₂, and *H*₃. The sequence of *H*₁ haplotype was identical to reference genome, in which tandem duplication of *endoPG* genes, *PGM* and *PGF*, was observed. *H*₂ haplotype possessed only *PGM* and lacked *PGF*. The 70 kbp



region containing *PG2*, *PGM*, *PGF*, and *NADHs* was deleted in H_3 haplotype. Gu et al. (2016) hypothesized that H_1 and H_2 haplotypes were dominant over H_3 haplotype, *PGM* conferred the melting texture, and *PGF*, which was present only in H_1 haplotype, was involved in freestone phenotype. The lack of both *PGM* and *PGF* in H_3 homozygote could result in the non-melting texture. Further investigations are required to confirm the function of *PGM* in H_2 and H_1 haplotypes and the roles of *PGM* and *PGF* in fruit trait.

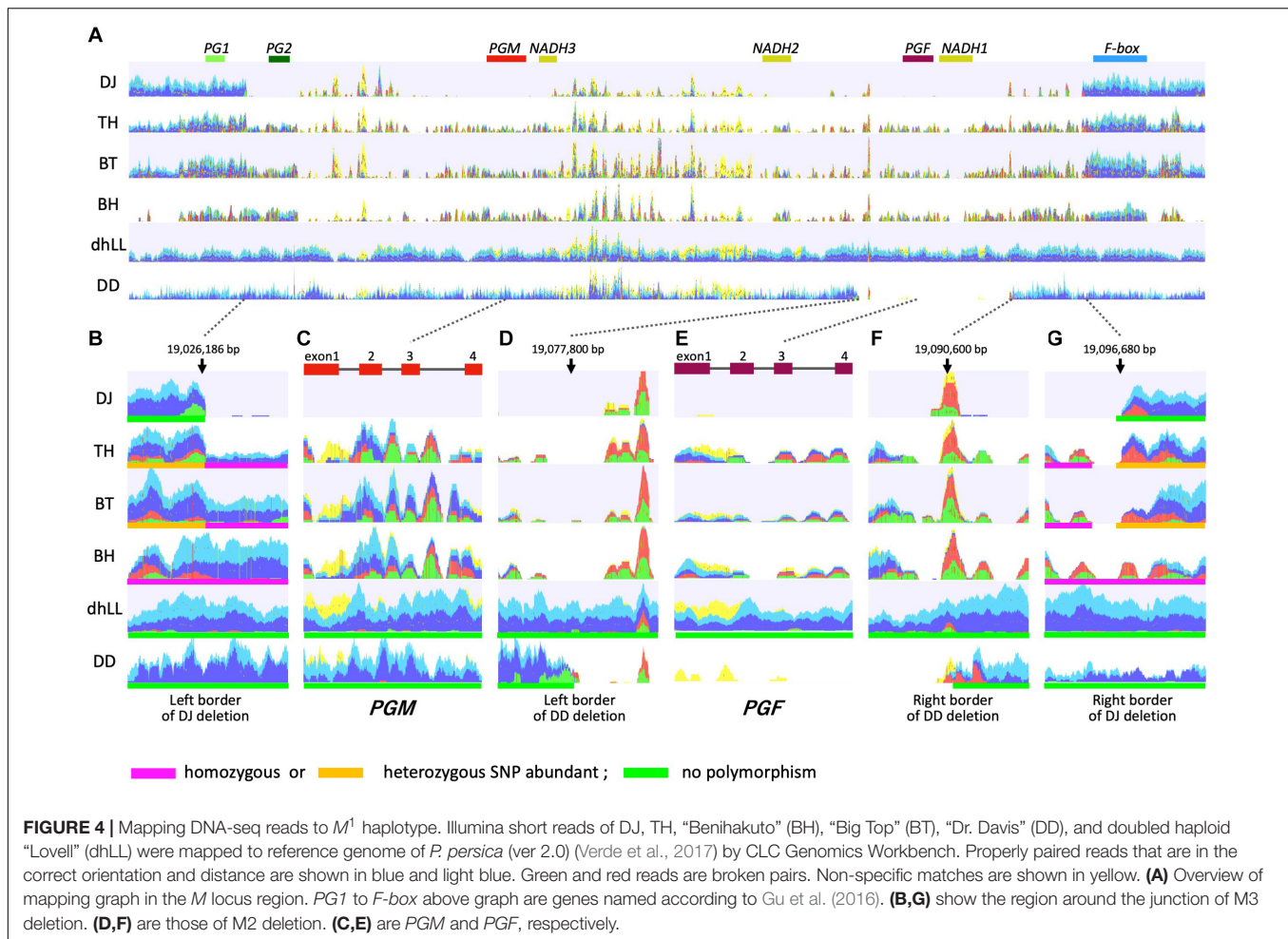
WGS of DJ and TH by Illumina was performed to investigate the *M* locus region (19.0–19.1 Mbp of chromosome 4) (Figure 4), and the mapping patterns were compared with those of three accessions with different flesh textures: dhLL of MF accession, DD of NMF accession, and BT of MF accession, which is categorized in slow softening peaches (Bassi and Monet, 2008; Ghiani et al., 2011; Morgutti et al., 2017). dhLL, an H_1 homozygote, was used for peach genome sequencing and the reads were mapped uniformly to *M* locus. The reads of DD were also mapped to the entire *M* locus region except the ~ 12 kbp region including *PGF* and *NADH1*. No or less reads were mapped to the ~ 12 kbp region, indicating that the region was deleted in DD (Figures 4D,F). The position and length indicated that the DD deletion unexpectedly corresponded to the region deleted in H_2 haplotype in Gu et al. (2016). The mapping patterns of DJ and TH were not the same as those of dhLL and DD, suggesting that DJ and TH possessed neither H_1 nor H_2 haplotype.

TH and BT showed similar mapping patterns and thus were expected to possess the same haplotypes (Figure 4). The DJ mapping results indicated that the genotype of DJ was not identical to those of TH and BT, but the three accessions were expected to share one haplotype. Mapping the pair reads of DJ to peach reference genome revealed many broken pairs around 19,026,186 and 19,096,680 bp (Figures 4A,B,G). Only a few reads were mapped between them, except for the many non-specific reads from other chromosomal regions that were mapped between *NADH3* and *NADH2*, the region named M1 insertion in this study (see below). Structural mutation analysis by CLC Genomics Workbench indicated that the region from 19,026,186 to 19,096,680 bp was deleted in DJ, suggesting that DJ is homozygote for the deleted haplotype identical to that reported as H_3 by Gu et al. (2016). Many broken pairs were found at the same position as DJ when mapped with TH and BT pair reads, indicating that one of the two haplotypes was H_3 (Figures 4A,B,G). The other haplotype was presumed to be an unidentified novel haplotype that cannot be predicted directly by mapping to reference genome. In TH and BT, SNPs were heterozygous in the outer region of H_3 deletion, whereas they were homologous in the inner region of H_3 deletion (Figures 4B,G and Supplementary Table S4). All SNPs in this region were homozygous in BH, a Japanese MF accession. In contrast, no SNP was detected in either dhLL or DD. In the region of *PGM* and *PGF*, the coverage of TH, BT, and BH was low and many SNPs and broken pair reads were observed (Figures 4C,E). Throughout *M* locus and its surrounding region, SNPs were hardly observed in dhLL, DD, and DJ, whereas many mutations were detected in TH, BT, and BH (Figure 4 and Supplementary Table S4), suggesting the existence of an unidentified haplotype in TH, BT, and BH.

Identification of M^0 Haplotype

Sequence polymorphism and mapping pattern indicated that the sequence and structure of the unidentified haplotype of TH, BT and BH was highly diverged from those of the reference sequence (M^1). We decided to obtain the unidentified haplotype sequence by *de novo* assembly. However, polymorphism shown in the *M* locus of TH had a negative effect on *de novo* assembly. As we found that BH was a homozygote of the unknown haplotype, *de novo* assembly with PE150 reads of BH was conducted and two contigs covering *M* locus were obtained. *PG1*, *PG2*, *PGM*, and *NADH* were located in one of the two contigs. The *F-box* gene was found in another contig. The haplotype composed of the two contigs was defined as M^0 according to the locus name. Haplotypes H_1 , H_2 , and H_3 in Gu et al. (2016) were renamed M^1 , M^2 , and M^3 , respectively, based on haplotype features, to avoid confusion and define the haplotypes precisely.

When the genome structure of M^0 was compared with M^1 sequence, the region corresponding to *PGF* was not found in M^0 and only one *NADH* was located on M^0 (Figure 5). The sequences were conserved among the two haplotypes but M^1 specific sequences were found in the region from *PG2* to *PGM* and the downstream region of *NADH3*. Many non-specific reads were mapped to the region spanning from *NADH3* to *NADH2* of M^1 haplotype, the region corresponding to M1



insertion described above (Figures 4, 5). The M^1 insertion was assumed to be translocated from another chromosomal region and inserted into *NADH* to disrupt it, because both *NADH3* and *NADH2* were partial and their structures appeared to be generated from one *NADH* gene divided at the third intron by the M^1 insertion (Supplementary Figures S3, S4 and $NADH3/2$ of Supplementary Figure S5).

The CDS sequence of *PGM* of M^0 ($PGM-M^0$) showed 99% similarity to those of *PGM* of M^1 ($PGM-M^1$) and *PGF* of M^1 . One amino acid substitution between $PGM-M^0$ and $PGM-M^1$ was found at residue 49, where Ser was substituted to Phe in $PGM-M^1$ (Supplementary Figure S6). The Ser at residue 49 of $PGM-M^0$ was conserved in other *Prunus* species. Amino acid sequence comparison between $PGM-M^0$ and *PGF* showed substitution of Ser for Thr at residue 269 in *PGF*, although it was not considered to have a significant effect on the function of the PG protein. The S49F substitution between f and fl alleles was reported by Peace et al. (2005) and Morgutti et al. (2017). However, because they did not perform resequencing analysis, it was not possible to understand the entire structure of the f haplotype and its origin. It was probable that f haplotype was the same as M^0 in this study. We further demonstrated that this M^0 haplotype is not a specific haplotype but a widely found haplotype in

various peach accessions, and plays an important role in MF phenotype determination.

DNA-seq reads of BH, TH, DJ, dhLL, DD, and BT were mapped to the reference “PpREF20 + M^0 ,” in which the M^0 haplotype sequence was added to peach genome sequence (Figure 5). Coverage graphs show that the reads of M^0 , M^1 , M^2 , and M^3 haplotypes could be classified clearly. The reads of BH (M^0M^0) were mapped only to M^0 haplotype and those of dhLL (M^1M^1) were also mapped only to M^1 haplotype. DJ (M^3M^3) and DD (M^2M^2) reads were mapped to M^1 haplotype except for the deleted region, as shown in Figure 4. The reads of TH (M^0M^3) and BT (M^0M^3) were mapped to both M^0 and M^1 haplotypes except for M^3 deletion.

Structural Variety of *M* Haplotype Identified by WGS Mapping Patterns and PCR Genotyping

It was demonstrated that WGS data were useful for the precise genotyping of *M* locus. Many WGS data of peach accessions were registered in the SRA database and mapped to “PpREF20 + M^0 ” to identify *M* genotype. We finally predicted *M* genotypes of 412 accessions from the WGS mapping pattern and/or by PCR

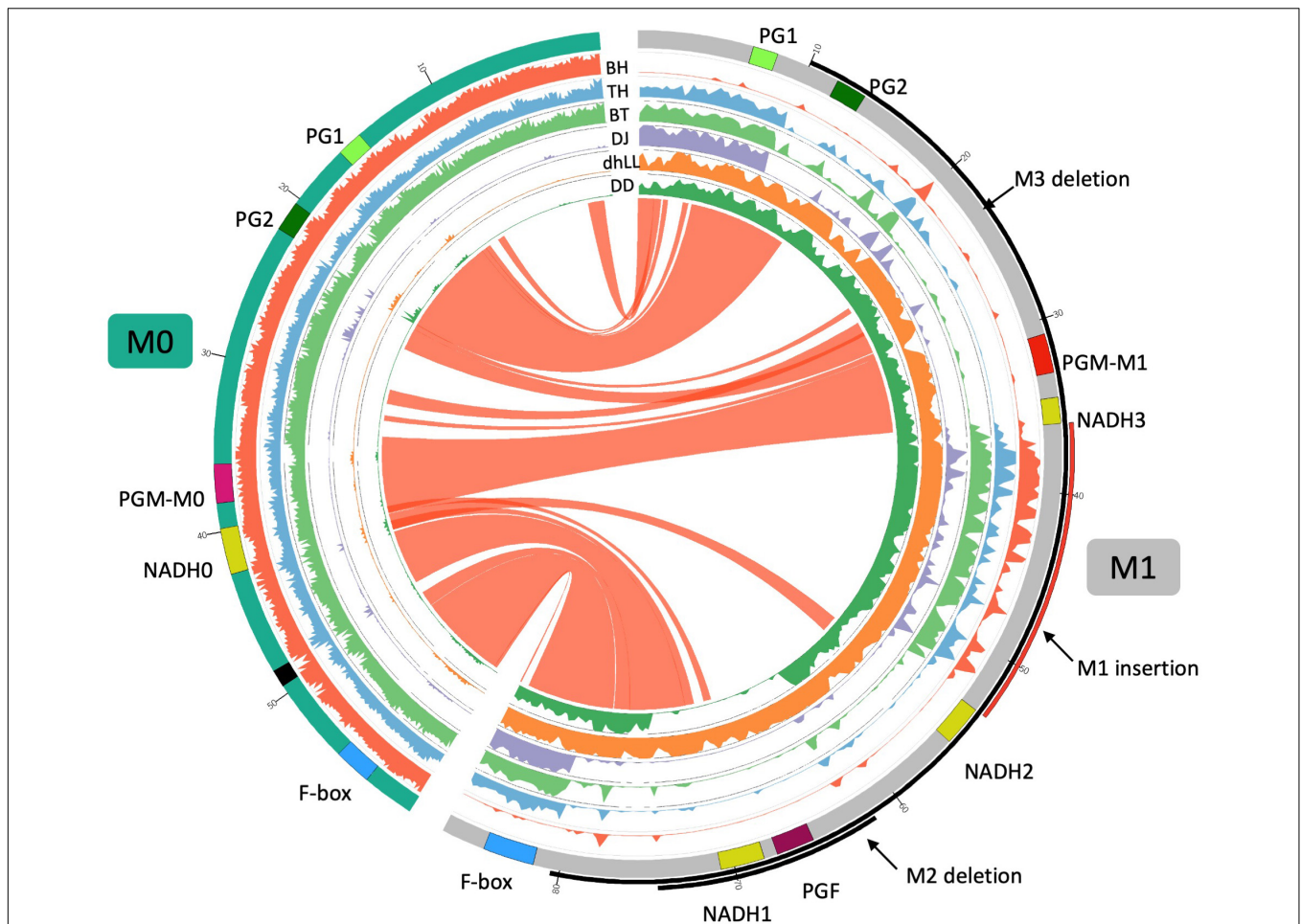


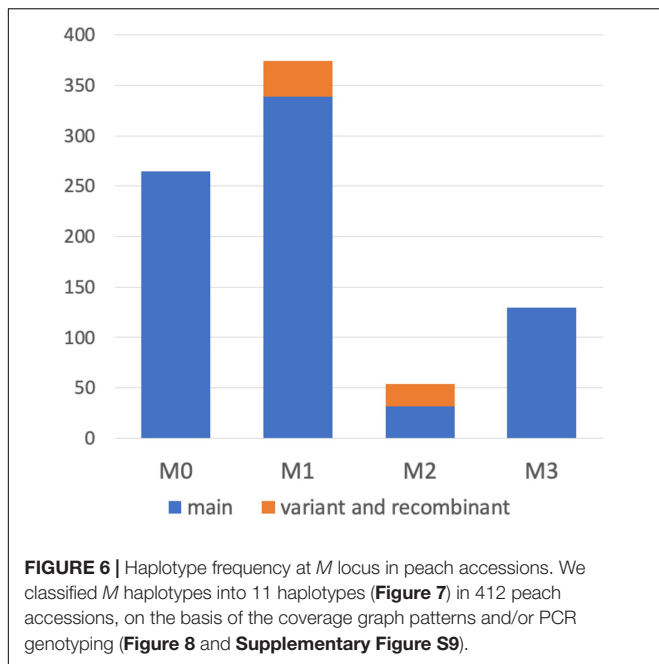
FIGURE 5 | Comparison of M^0 and M^1 haplotypes. Inner six tracks are coverage graphs of DNA-seq reads of BH TH, BT, DJ, dhLL, and DD. Ribbons link similar regions between two haplotypes. M^0 haplotype consists of two contigs connected by N (black in the chromosome track). The nucleotide at 19,016,188 bp of Pp04 chromosome is positioned as + 1 in M^1 haplotype. *PGM* of M^0 haplotype is similar to *PGM* of M^1 but not identical. We named those *PGMs* $PGM-M^0$ and $PGM-M^1$, respectively. *NADH0* is *NADH* of M^0 haplotype and seems to be an intact gene as described in **Supplementary Figures S3–S5**.

genotyping. M^0 and M^1 haplotypes were the most popular in the peach accessions analyzed (**Figure 6** and **Supplementary Table S5**). On the other hand, the frequency of M^2 haplotype was very low. In addition to the four main haplotypes, M^0 , M^1 , M^2 , and M^3 , we found variant-type haplotypes and chimeric haplotypes. The former haplotypes exhibited deletion in the region different from those found in M^2 and M^3 , whereas the latter haplotypes appeared to be generated by the recombination between M^0 and M^1 (**Figure 6**). In total, 11 haplotypes were structurally identified at *M* locus (**Figure 7**). They were first classified into M^0 to M^3 on the basis of the existence of $PGM-M^0$, $PGM-M^1$, and *PGF*; the haplotype containing only $PGM-M^0$ is M^0 ; the haplotype containing $PGM-M^1$ and *PGF* was M^1 ; the haplotype containing only $PGM-M^1$ was M^2 ; and the haplotype containing neither *PGM* nor *PGF* was M^3 . Furthermore, variants and recombinant types of haplotypes were identified from structural variations and such characters as b, c... or r1, r2... were added to their names, respectively.

Although no significant structural change in gene composition was detected, the sequence variation was found in the accessions with M^0 haplotype, when analyzed on the basis of the mapping patterns of DNA-seq reads of TH. The insertion, whose length was unknown, was found in the 1.8 kbp upstream region of $PGM-M^0$, and SNPs were also detected in $PGM-M^0$, one of which was located in CDS and led to a synonymous substitution (**Supplementary Figure S7**). It was expected that M^0 was also diversified. However, we regarded both types of M^0 as M^0 in this study because no changes in gene composition (structural feature as haplotype) and no amino acid substitutions were found.

M^0 Haplotype Was Widely Spread Among MF Accessions

We designed primers for PCR genotyping on the basis of the sequence variations at the third intron of *PGM* and *PGF* and the *M* haplotype structural differences (**Figure 8**, **Supplementary Figure S8**, and **Supplementary Table S3**). The structural

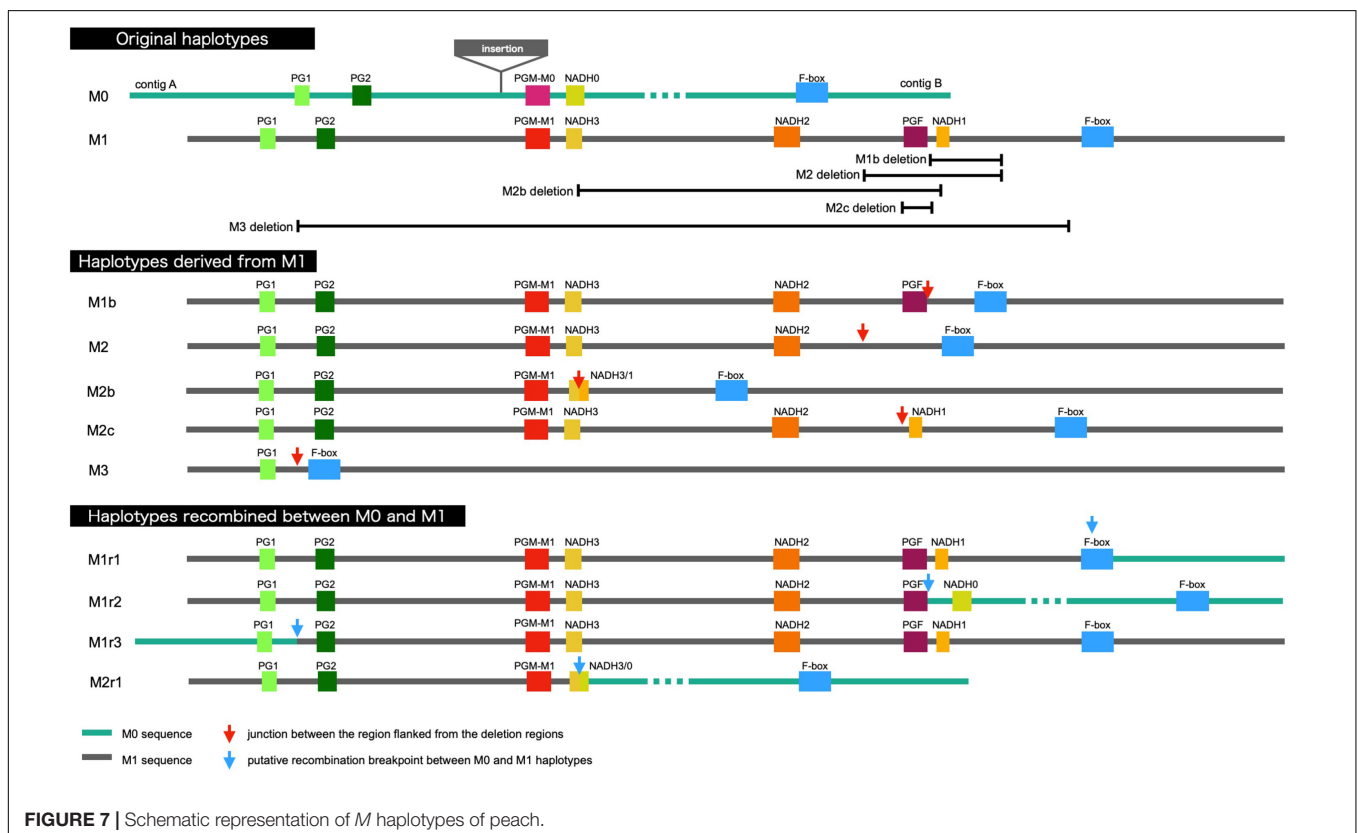


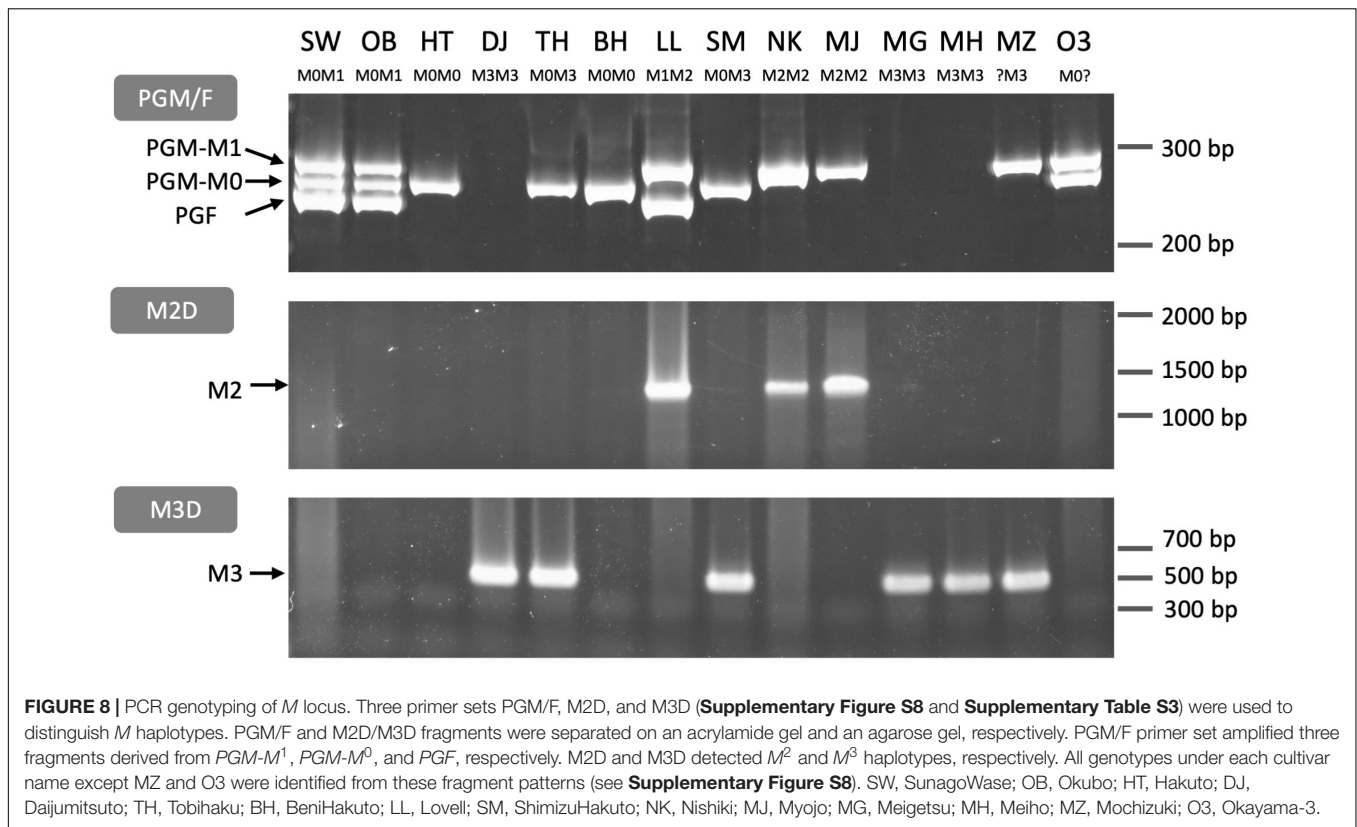
variations and the *PGM* and *PGF* compositions of *M* haplotypes identified in this study indicated that the four main haplotypes could be classified using three primer sets, PGM/F, M2D, and M3D. PGM/F primer set detected the indel at the third intron of

PGM and *PGF*, and three different fragment sizes were amplified (Figure 8). The upper fragment was derived from *PGM-M*¹, the lower one was from *PGF*, and the middle one was from *PGM-M*⁰. When the middle fragment was amplified, the accession possessed *M*⁰ haplotype. From *M*¹ haplotype, both the upper and the lower fragments should be amplified. When the lower fragment was not amplified and only the upper one was amplified, this meant that only *PGM-M*¹ was amplified, showing that the accession had *M*² haplotype. The genotyping results obtained with the PGM/F primer set could be confirmed by amplification with the M2D primer set that detects the deletion on *M*². Because no fragment was amplified from *M*³ with the PGM/F primer set, the M3D primer set, which amplifies the junction of *M*³ deletion, should be useful to identify *M*³ haplotype.

The three primer sets were used to genotype 14 accessions. The *M* genotypes of six accessions, “Okubo” (OB), DJ, TH, BH, LL, and “Myojo” (MJ), were predicted from the mapping patterns of WGS data, which were re-confirmed by PCR genotyping. In the other eight accessions, we found inconsistent amplification patterns in “Mochizuki” (MZ) and “Okayama-3” (O3). These two accessions were expected to have *M*² haplotype judging from the result that the PGM/F primer set amplified *PGM-M*¹ but not *PGF*. However, no amplification was observed in M2D. These results suggested that *M*² haplotype of MZ and O3 was a variant type of *M*². Indeed, an additional primer set showed that they have *M*^{2b} (Supplementary Figure S9).

“Hakuto” (HT), a progeny of “Chinese Cling” (CC), was mainly used as germplasm for MF peach breeding in Japan





(Supplementary Figure S10A; Yamamoto et al., 2003a,b). PCR genotyping showed that HT was a homozygote of *M*⁰, indicating the possibility that *M*⁰ haplotype had been spread among Japanese peaches. All the major Japanese cultivars tested in this study were found to have *M*⁰ haplotype (Supplementary Figure S10B). All cultivars except OB and “ShimizuHakuto” (SM) were homozygotes of *M*⁰. SM was a typical MF cultivar in Japan (Yamamoto et al., 2003b), and its genotype was *M*⁰*M*³, the same as that of TH (Figure 8).

*M*² and *M*³ Could Confer NMF Phenotype

DJ was an *M*³ homozygote and did not have *PGM* and *PGF*. Thirty seven *M*³ homozygotes were identified in this study. Flesh textural phenotypes of 16 out of 37 accessions were reported, and 12 accessions were reported as NMF except those whose flesh texture was only reported as Supplementary Data in Cao et al. (2016) (Table 1). This may support our conclusion that *M*³ haplotype was likely involved in the determination of non-softening postharvest property in DJ. *M*² haplotype, in which only *PGM-M*¹ was located, also appeared to confer the NMF phenotype, unlike *M*⁰ and *M*¹ haplotypes. In this study, we found 22 homozygotes for *M*² including variant types, 11 of which had fruit textural report(s), and all 11 were reported as NMF (see reference in Table 1). Only NJF16 accession had *M*²*M*³ combination as well as phenotype report. NJF16 was reported to be NMF peach (Clark and Finn, 2010). MZ was *M*^{2b}*M*³ that had only *PGM-M*¹ as confirmed by PCR genotyping, and is a well-known Japanese NMF cultivar (Yoshioka et al.,

2011). All together, these findings suggest that *PGM-M*¹ may not be functional. On the other hand, *PGM-M*⁰ and *PGF* seemed to confer the MF phenotype dominantly because flesh texture of *M*⁰*M*² (“Tsukuba 86”), *M*⁰*M*^{2b} (O3), *M*⁰*M*³ (TH, SM, BT, and CC), *M*¹*M*² (LL), and *M*¹*M*³ [“Georgia Bell” (GB)] was MF (Table 1). “Early Gold” (EG) was identified as *M*¹*M*¹ on the basis of the mapping pattern of reads from the SRA database (Supplementary Table S6), despite that the flesh texture was considered NMF (Yoshida, 1981). We suspected that the reads of EG registered in SRA were confused with those of the other accessions. This is because “Nishiki” (NK) (*M*²*M*²), an NMF accession, was the parent of EG (Yoshida, 1981) and one of EG haplotypes was supposed to be *M*².

M Locus Structure in *Prunus* Species

The structure of *M* locus was identified from reference genome sequences of other *Prunus* species, including *P. mira*, *P. kansuensis*, almond (*P. dulcis*), apricot (*P. armeniaca*), Japanese apricot (*P. mume*), sweet cherry (*P. avium*), and Yoshino cherry (*P. x yedoensis*; called “Sakura” in Japan), and compared with the four main haplotypes of peach structurally identified in this study (Figure 9 and Supplementary Figure S11). *PGM* and *PGF* were found in the “Lauranne” genome (PdLN) of almond, which belongs to subgenus *Amygdalus* together with peach, indicating that the PdLN *M* haplotype was similar to peach *M*¹ haplotype. As shown in *M*¹ of peach, *NADH* located downstream of *PGM* in PdLN was broken by an insertion

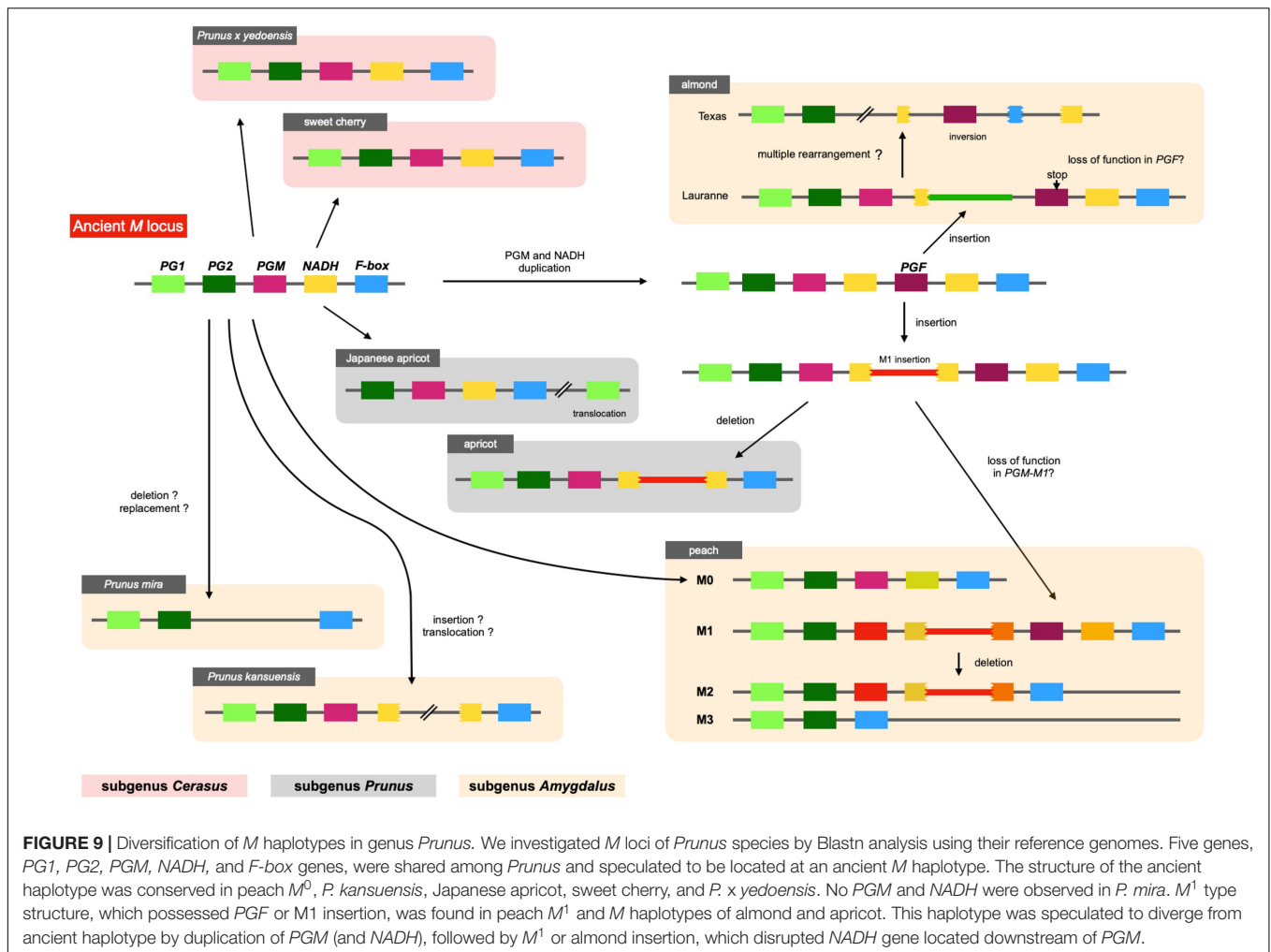
TABLE 1 | Flesh texture of M^2 or M^3 homozygotes and heterozygotes.

Cultivar	Haplotype	PGM-M ⁰	PGM-M ¹	PGF	Flesh texture	References
M2 homozygote						
Dr. Davis	M2M2	No	Yes	No	Non-melting	Peace et al., 2005
Phillips	M2M2	No	Yes	No	Non-melting	Cao et al., 2016 Old canning peach cultivar (Davis, 1937), Some progenies were non-melting (Wang and Lu, 1992; Font i Forcada et al., 2013)
Oro A	M2M2	No	Yes	No	Non-melting	Morgutti et al., 2017
Carson	M2M2	No	Yes	No	Non-melting	Infante et al., 2011; Font i Forcada et al., 2013
NJC105	M2M2	No	Yes	No	Non-melting	Pan et al., 2015
Myojo	M2M2	No	Yes	No	Non-melting	Gu et al., 2016
Nishiki	M2M2	No	Yes	No	Non-melting	Haji et al., 2005. Parent of Early Gold (Yoshida, 1981)
Loadel	M2M2	No	Yes	No	Non-melting	Font i Forcada et al., 2013
G. Klamt	M2M2	No	Yes	No	Non-melting	Font i Forcada et al., 2013
Everts	M2M2	No	Yes	No	Non-melting	Font i Forcada et al., 2013
Golden Queen	M2bM2b	No	Yes	No	Non-melting	Font i Forcada et al., 2013
M3 homozygote						
Daijimitsuto	M3M3	No	No	No	Non-melting	This study
Dawangzhuang Huang Tao	M3M3	No	No	No	Non-melting	Cao et al., 2016
Maria Serena	M3M3	No	No	No	Non-melting	Font i Forcada et al., 2013
Long 1-2-4	M3M3	No	No	No	Non-melting	Yoon et al., 2006
NJC77	M3M3	No	No	No	Non-melting	Pan et al., 2015
NJC47	M3M3	No	No	No	Non-melting	Pan et al., 2015
Meiho	M3M3	No	No	No	Non-melting	Personal communication
Ying Zui Tao	M3M3	No	No	No	Non-melting	Cao et al., 2016
Xi Jiao 1	M3M3	No	No	No	Non-melting	Cao et al., 2016
Yu Bai	M3M3	No	No	No	Non-melting	Zhang et al., 2019
Rou Pan Tao	M3M3	No	No	No	Non-melting	Yoon et al., 2006
Zhang Huang 9	M3M3	No	No	No	Non-melting	Cao et al., 2016
Fen Ling Chong	M3M3	No	No	No	Melting	Cao et al., 2016
Mai Huang Pan Tao	M3M3	No	No	No	Melting	Cao et al., 2016
Tsukuba 85#	M3M3	No	No	No	Melting	Cao et al., 2016
Zhong You Pan Tao 2	M3M3	No	No	No	Melting	Cao et al., 2016
Heterozygote						
Mochizuki	M2bM3	No	Yes	No	Non-melting	Yoshioka et al., 2011
NJF16	M2M3	No	Yes	No	Non-melting	Clark and Finn, 2010
Okayama-3	M0M2b	Yes	Yes	No	Melting	Cao et al., 2016. A germplasm for canning cultivar breeding (Yoshida, 1981)
Tsukuba 86	M0M2	Yes	Yes	No	Melting	Cao et al., 2016
Big Top	M0M3	Yes	No	No	Melting	Bassi and Monet, 2008. Flesh softening was very slow
Tobihaku	M0M3	Yes	No	No	Melting	This study
Chinese Cling	M0M3	Yes	No	No	Melting	Pan et al., 2015
Shimizu Hakuto	M0M3	Yes	No	No	Melting	Gu et al., 2016
Lovell*	M1M2	No	Yes	Yes	Melting	Some progenies were non-melting (Font i Forcada et al., 2013)
Georgia Bell	M1M3	No	Yes	Yes	Melting	Some progenies** were non-melting (Peace et al., 2005)

Twenty-two M2 homozygotes, including variant and recombinant types, and 37 M3 ones were found in this study. Accessions whose flesh texture was reported are listed in this table.*This "Lovell" was not doubled haploid used for genome sequencing.**Includes offspring from self-pollination and cross of "Dr. Davis" and "Georgia Bell."

sequence, although this insertion sequence was not similar to the M1 insertion. *F-box* and *NADH* were pseudogenes, probably due to multiple genome rearrangements occurring in almond "Texas" genome (PdTX). One *endoPG* was found in addition

to *PG1* and *PG2*, and it was expected to be *PGF*, because *PGFs* in PdLN and PdTX shared amino acid substitutions specific to them and genomic sequence similarity was found not only in the gene region, but also in the intergenic region



flanking them. A frameshift mutation was found in *PdLN-PGF*, indicating that *PdLN-PGF* did not function. The absence of this mutation in *PdTX* suggests that the mutation in *PdLN-PGF* occurred after the haplotype diverged. No tandem duplications of *PGM*, *PGF*, and $M1$ insertions were observed in *P. mira* or *P. kansuensis*. *NADH* appeared to be a fragmented structure in *P. kansuensis*, but because disrupted exons were located at different contigs in the draft genome, their actual relationship was unclear. *PGM*, *PGF*, and *NADH* were not present in *P. mira* genome.

In subgenus *Amygdalus*, the $M1$ insertion was found only in peach. However, a sequence similar to the $M1$ insertion was found in apricot of subgenus *Prunus*. The insertion also disrupted *NADH*, which was located downstream of *PGM*. These findings implied that the two insertions originated from the same event (haplotype), and that this insertion event occurred before the divergence of subgenera *Amygdalus* and *Prunus*. A structure similar to M^0 was found in Japanese apricot (*P. mume*) of subgenus *Prunus*. *PG2*, *PGM*, intact *NADH*, and *F-box* were clustered in *P. mume* haplotype, but *PG1* was translocated to the downstream region to *M* locus. Sweet cherry and Yoshino cherry belong to subgenus *Cerasus*, which is far from

subgenus *Amygdalus* (Chin et al., 2014). Their *M* haplotype structure and gene composition were similar to those of peach M^0 haplotype.

DISCUSSION

Different Postharvest Properties of TH and DJ

In this study, first, the postharvest properties of ultra-late maturing peach cultivars TH and DJ were investigated. Generally, peach is considered to be a climacteric fruit in which ripening-related phenomena, such as accelerated endogenous ethylene biosynthesis and fruit softening, were reported to be controlled by ethylene (Liguori et al., 2004; Hayama et al., 2006; Liu et al., 2018). TH exhibited the characteristics of normal MF peach fruit, including rapid fruit softening leading to MF texture associated with appropriate level of endogenous ethylene production. In contrast, DJ did not soften at all even though significant ethylene production was observed. From their sugar contents and pH-values at day 0, it was confirmed that DJ fruit used in this study were not harvested at too early maturity

stage to be ripen normally (**Supplementary Figure S1**). It seemed that DJ possessed the ability to produce ripening-related ethylene but lacked the ability to be softened in response to the ethylene. The lack of softening ability in response to ethylene in DJ was supported by the continuous propylene treatment. Propylene, instead of ethylene, treatment has been used to monitor endogenous ethylene production in parallel to other ripening-related changes (McMurchie et al., 1972). As much as 5,000 ppm of propylene was used for treatment in this study. According to previous reports, this concentration of propylene is equivalent to 50 ppm of ethylene and is sufficient to induce ethylene response in climacteric fruits (Burg and Burg, 1967; McMurchie et al., 1972). Indeed, in peach fruit treated with 500–5,000 ppm of propylene, induction of autocatalytic ethylene production and dramatic fruit softening were reported (Yoshioka et al., 2010; Liu et al., 2018). In this study, DJ exhibited only a slight decrease in flesh firmness and maintained almost similar firmness to that at harvest even after 7 days of continuous propylene treatment. As TH showed dramatic softening by the propylene treatment, it is suggested that the propylene treatment in this study is capable of inducing ethylene response in peach and that DJ has a non-softening characteristic in response to both endogenous and exogenous ethylene/propylene.

Involvement of *M* Locus in Determining Different Postharvest Properties of DJ and TH

The genetic background of DJ and TH and its relationships with other cultivars having long storability and/or shelf lives are unknown. One of the peach strains reported to have a long shelf life is SH peach (Haji et al., 2005). SH peaches, however, are characterized by the absence of ethylene production (Tatsuki et al., 2006). It is reported that ethylene sensing is normal in SH peaches and the fruit soften rapidly with exogenous ethylene or propylene treatment (Haji et al., 2003; Yoshioka et al., 2010), in contrast to DJ. A similar ripening characteristic observed in DJ has been reported in early harvest fruit of SR peaches (Brecht and Kader, 1984). In SR peaches harvested at an earlier date than the optimum harvest date, autocatalytic ethylene production was induced with or without propylene treatment whereas flesh firmness decreased quite slowly. However, DJ is phenotypically different from SR peaches in that it bears large fruit with red coloration, as shown in **Figure 2**, whereas SR fruit do not show normal ripening in terms of fruit size and coloration (Giné-Bordonaba et al., 2020). In agreement with these phenotypical differences between DJ and SH and/or SR peaches, the genomic sequences of DJ and TH did not exhibit any significant differences and/or mutations in the candidate causal genes for these specific strains, *YUCCA flavin mono-oxygenase* (Pan et al., 2015; Tatsuki et al., 2018) and *NAC transcription factor* (Eduardo et al., 2015; Nuñez-Lillo et al., 2015; Meneses et al., 2016) genes (data not shown).

On the other hand, significant differences between DJ and TH were found with regard to genomic sequences at *M* locus, which has been reported to control MF and NMF textures (Bassi and Monet, 2008; Gu et al., 2016). *M* locus is composed of

two tandem *endoPG* genes, *PGM* and *PGF* (Gu et al., 2016). Resequencing analysis revealed that DJ is a homozygote of the haplotype that lacks both *PGM* and *PGF*, designated as M^3 in this study, whereas TH is a heterozygote of M^3 and a structurally uncharacterized haplotype that possesses *PGM* ($PGM-M^0$) but not *PGF*, designated as M^0 in this study (**Figures 4, 5**). Many reports have demonstrated that high level of enzymatic activity, protein accumulation, and gene expression of *endoPG* are observed only in MF, and supported the involvement of *endoPG* in the determination of the flesh texture (reviewed in Bassi and Monet, 2008). Thus, it is considered that DJ is a member of NMF peaches. NMF peaches are known to be firm at maturity and to soften slowly during ripening without melting. Different from DJ, it was reported that softening progressed steadily during postharvest ripening in NMF peaches (Fishman et al., 1993; Yoshioka et al., 2011) and thus, the possible involvement of a number of factors in the non-softening property of DJ other than the lack of *endoPG* genes cannot be excluded. Nevertheless, it was indicated that the non-softening postharvest property of DJ is attributed to the lack of *endoPG* genes at *M* locus. The rapid softening property of TH is due to the presence of newly characterized M^0 haplotype ($PGM-M^0$ gene) in TH genome. This was further confirmed by the re-evaluation of *M* haplotype in relation to flesh textural phenotypes in 412 accessions, as described below.

Re-evaluation of *M* Locus in Relation to Flesh Textural Phenotypes

In this study, we revealed that M^0 was not only a unique *M* haplotype as shown in TH, but also a widely spread haplotype in MF accessions, particularly popular peach cultivars grown in Japan, and was responsible for the MF phenotype in these accessions (**Figure 6, Supplementary Figure S10B, and Supplementary Table S5**). Based on the results obtained from the re-evaluation of *M* locus in 412 accessions in relation to flesh textural traits, we proposed the scenario in which four *M* alleles/haplotypes, M^0 to M^3 , were involved in the determination of flesh texture, with M^0 and M^1 dominantly controlling MF texture over M^2 and M^3 .

Various alleles/haplotypes have been proposed for *M* locus. The correspondence of *M* alleles/haplotypes in previous studies to those in this study is summarized in **Supplementary Tables S7, S8**. Peace et al. (2005) classified *endoPGs* at *M* locus into four alleles, F, f1, f, and null, on the basis of the results obtained from germplasm derived from peach cultivars GB and DD with f allele being hypothesized to be segregated via outcross from an unknown origin. Morgutti et al. (2017) assumed the same four haplotypes F, f1, f, and f_{null} by referring to Peace's classification and further found two variations, PG^{SH} and PG^{BT} , in f haplotype. The haplotype structures of H₁, H₂, and H₃ reported by Gu et al. (2016) corresponded to those of F, f1, and f_{null} alleles, respectively, although the haplotype corresponding to f was not reported by Gu et al. (2016). In this study, we structurally identified four main haplotypes M^0 to M^3 . Judging from S49F substitution and indel at the third intron detected between $PGM-M^0$ and $PGM-M^1$, M^0 appeared to be identical to f haplotype. However, the derivation of

$f(M^0)$ haplotype assumed in this study was different from that in Morgutti et al. (2017), in which $f(M^0)$ was expected to be derived from $F(M^1)$ via $fl(M^2)$. We detected sequence diversifications and large structural differences between M^0 and M^1/M^2 and assumed that M^0 was not derived from M^1/M^2 directly. This assumption was supported by a structural comparison of M loci of other *Prunus* species (Figure 9). A similar specific structure to peach M^1 , such as M1 insertion and/or tandem duplication of *endoPG*, was found in M haplotypes of almond and apricot. On the other hand, there was no insertion to disrupt *NADH* in peach M^0 or M haplotypes of the Japanese apricot, sweet cherry, and *P. x yedoensis*. These findings suggested that the ancestral haplotypes of M^0 and M^1 diverged relatively early, before subgenus divergence, and evolved independently of each other. On the other hand, we could not find any SNP-level variation among M^1 , M^2 , and M^3 (Supplementary Table S4), suggesting that the divergence of M^1 into M^2 and M^3 occurred relatively recently after *P. persica* speciation. It was also suggested that M^2 did not lead to M^1 but rather M^2 was derived from M^1 . This might be supported by the fact that the frequencies of M^2 and M^3 were much lower than that of M^1 at least in the accessions investigated in this study (Figure 6). In this study, we showed 11 haplotypes in total (Figure 7), but more haplotypes are expected to exist. We only examined reference genomes in *Prunus* species other than *P. persica*. Considering the divergence of M haplotype before speciation, it would not be surprising to find other species harboring haplotypes similar to both M^0 and M^1 haplotypes.

Gu et al. (2016) did not consider the presence of *PGM-M^0* (f allele) and defined H_2 as the sole haplotype harboring *PGM* but not *PGF* because they attempted to distinguish each haplotype on the basis of copy number of *endoPG* genes quantified by qPCR. Therefore, not only M^2 but also M^0 was genotyped as H_2 in Gu et al. (2016). This misgenotyping of M^0 as H_2 produced results that included incongruity between genotype and phenotype as M^0 (*PGM-M^0*) and M^2 (*PGM-M^1*) were likely to have different effects on flesh texture. For example, the genotyping in Gu et al. (2016) identified that SM and “Hakuho” (HH), both of which are popular MF cultivars in Japan, were H_2H_3 and H_2H_2 , respectively. Supposing *PGM-M^1* on H_2 is not functional, as assumed in this study, SM and HH should be NMF. Conversely, supposing H_2 (M^2) is a dominant haplotype that determines MF texture, as assumed by Gu et al. (2016), the H_2H_2 genotype shown in DD, “OroA” (OA), and MZ cannot explain their NMF phenotypes (Peace et al., 2005; Morgutti et al., 2006, 2017; Yoshioka et al., 2011).

Re-evaluation of M locus in association with MF/NMF phenotypes in this study revealed that M^0 and M^1 were likely to function dominantly over M^2 and M^3 . To our knowledge, M^0M^3 was linked to MF, as shown in TH, SM, and BT. LL (M^1M^2) was also reported to exhibit MF phenotype (Font i Forcada et al., 2013), whereas NJF16 (M^2M^3) and MZ ($M^{2b}M^3$) had NMF phenotype (Clark and Finn, 2010; Yoshioka et al., 2011; Table 1). Although *PGM-M^1* was present in M^2 , its expression level seemed to be suppressed as reported in OA, whose genotype was determined as M^2M^2 in this study (Morgutti et al., 2006). Thus, the low expression of *PGM-M^1* was consistent

with the feature of M^2 , namely, recessive against M^1 and M^0 , and comparable to M^3 . The hypothesis cannot be excluded that M^2 haplotypes in NMF accessions are specific haplotypes possessing additional mutation(s) that result in the disruption of M^2 function. The sequences of *PGM-M^1* and its surrounding region on M^2 and M^1 haplotypes were identical with each other. As it was predicted that M^2 was generated from M^1 by deletion of the region including *PGF*, it seemed reasonable to consider that *PGM-M^1* had lost its function before the emergence of M^2 haplotype and, thus M^2 haplotype in general was not functional. This prediction was supported by Morgutti et al. (2017), who reported that all accessions harboring *flf* (M^2M^2) or *flf_{null}* (M^2M^3) exhibited NMF phenotype, as well as previous reports showing the existence of accessions exhibiting NMF phenotype but not completely lacking *endoPG* genes (Lester et al., 1994, 1996; Callahan et al., 2004; Peace et al., 2005; Morgutti et al., 2006).

It was hypothesized that two tandem *endoPG* genes at M locus, *PGM*, and *PGF*, were responsible for peach flesh texture regulation (Gu et al., 2016). In this study, we suggested that *PGM-M^0* and *PGF* in particular would affect flesh textural quality whereas *PGM-M^1* would have no effect. Considering the lack of sequence diversification and the relatively recent divergence between M^1 and M^2 , it would not be possible that *PGM-M^1* on M^1 retains its function. Although 11 haplotypes were characterized in this study, it might not be necessary to identify correctly all the haplotypes in order to estimate flesh textural quality in a breeding program. Only an analysis to confirm the presence of *PGM-M^0* and *PGF* should be sufficient. This means we only need to test whether the *PGM/F* primer set (Figure 8 and Supplementary Figures S9, S10B) amplifies *PGM-M^0* or *PGF* fragments to estimate MF/NMF phenotypes in individual accessions and progenies.

M locus is strongly linked to freestone/clingstone (F) locus. It seems that *PGM-M^0* is not responsible for the determination of F trait because most M^0M^0 and M^0M^3 accessions have clingstones. Gu et al. (2016) hypothesized that not *PGM* but only *PGF* on H_1 (M^1) haplotype is associated with the freestone phenotype. We re-evaluated the relationship between M genotypes and reported freestone/clingstone phenotypes. We found some accessions harboring M^1 haplotype but being reported to have not freestone but clingstone phenotype (data not shown). Further studies are required to unravel the role of *PGF* in the regulation of stone adhesion.

The classification of M haplotypes based on genomic structure and the re-evaluation of M locus in association with flesh melting traits in this study are expected to provide valuable information for studies on controlling fruit softening and textural quality. For example, BT is a well-known cultivar having slow softening behavior, but reaches MF texture at full maturity (Bassi and Monet, 2008; Ghiani et al., 2011). The M genotype of BT was found to be M^0M^3 in this study, which was the same as that of SM, a famous Japanese MF cultivar that softens rapidly (Yamamoto et al., 2003b). Therefore, we suggest that the slow softening behavior of BT is controlled by loci other than M locus. Even with the re-evaluated genotypes in this study, there are few incongruities between M genotypes and MF/NMF phenotypes

(**Supplementary Table S6**). These incongruities may be due to different conditions and definitions for phenotyping flesh texture among experiments and/or specific mutation(s) that occurred in particular accessions, as well as the involvement of other loci. Further studies addressing the reason for these incongruities are expected to uncover mechanism(s) that determine flesh texture and fruit softening and to improve our understanding of factors related to long shelf life.

CONCLUSION

We found that two ultra-late maturing cultivars, DJ and TH, showed different postharvest properties. DJ did not soften at all during ripening in spite of significant ethylene production, whereas TH showed rapid fruit softening leading to MF texture. Resequencing analyses of DJ and TH demonstrated that DJ was a homozygote of *M* haplotype designated as M^3 and lacked two tandem *endoPG* genes, *PGM* and *PGF*, at *M* locus. On the other hand, TH was a heterozygote of M^3 and a structurally unidentified haplotype designated as M^0 that consisted of only *PGM-M*⁰ and was responsible for determining MF texture. Further classification of *M* haplotypes in 412 peach accessions revealed four main haplotypes: M^0 ; M^1 consisting of *PGM-M*¹ and *PGF*; M^2 consisting of *PGM-M*¹ and M^3 ; and M^0 was widely spread among MF accessions. We proposed the scenario that combinations of M^0 to M^3 determined flesh texture, and M^0 and M^1 dominantly controlled MF texture over M^2 and M^3 . These suggested the possibility that *PGM-M*⁰ and *PGF* could confer MF phenotype and *PGM-M*¹ of M^1 and M^2 haplotypes may have lost its function. This scenario was supported by the evolution history of each *M* haplotype assumed from the structural features of *M* locus in *Prunus* species, in which the ancestral haplotypes of M^0 and M^1 diverged before subgenus divergence and evolved independently of each other, whereas M^2 and M^3 were assumed to be derived from M^1 in recent age by deletion mutations.

DATA AVAILABILITY STATEMENT

The datasets analyzed for this study can be found in the DDBJ Sequenced Read Archive database (<https://www.ddbj.nig.ac.jp/dra/index-e.html>), accession numbers DRR248809-DRR248811 and DRR249197-DRR249201. The contigs A and B of M^0 haplotype will appear in the DDBJ/EMBL/GenBank databases under the accession numbers LC592228 and LC592229, respectively.

AUTHOR CONTRIBUTIONS

RN, TK, KU, and FF designed the study and drafted the manuscript. YF, DT, and MS performed sampling and phenotyping. RN, TK, YF, KA, and SW investigated postharvest ethylene production and flesh firmness. KU, RN, TK, and TA analyzed the genomic sequences of peach accessions and determined the genotypes of *M* locus in various peach accessions.

All authors have contributed to manuscript revision and have read and approved the submitted version.

FUNDING

This work was supported in part by the Ministry of Education, Culture, Sports, Science and Technology of Japan (Grant-in-Aid for Scientific Research No. 18H02200 to RN).

ACKNOWLEDGMENTS

Computations were partially performed on the NIG supercomputer at ROIS National Institute of Genetics.

SUPPLEMENTARY MATERIAL

The Supplementary Material for this article can be found online at: <https://www.frontiersin.org/articles/10.3389/fpls.2020.554158/full#supplementary-material>

Supplementary Figure 1 | Soluble solids contents and juice pH in postharvest TH and DJ. Postharvest changes in (A–C) soluble solids content and (D–F) juice pH in TH and DJ fruit grown in Okayama Prefecture and DJ grown in Fukushima Prefecture Japan. In (A, D), TH were harvested on November 7 from a commercial orchard in Okayama Prefecture, Japan and held at 25°C for 21 days. In (B, E), DJ from Okayama were harvested on October 12 from the Research Farm of Okayama University, Japan and held at 25°C for 21 days. In (C, F) DJ from Fukushima were harvested on October 22 from a commercial orchard in Fukushima Prefecture, Japan, followed by 2-day transport at ambient temperature to Okayama University, where fruit were held at 25°C for 21 days. Fruit were harvested at commercial maturity. Each point in (A, B, D, E) and in (C, F) represents the mean value of three and four fruits, respectively. Vertical bars indicate \pm SE ($n = 3-4$). Statistical analysis was conducted by Tukey's test after one-way ANOVA. Different letters indicate significant differences among measurement days by Tukey's multiple comparison test ($p < 0.05$).

Supplementary Figure 2 | Ethylene production in propylene treated TH and DJ. Effect of propylene treatment on postharvest ethylene production in (A) TH and (B) DJ fruit. Harvested fruit were treated with 5,000 ppm of propylene continuously for 7 days. Ethylene production was measured on days 0, 3, and 7. For (B) DJ, fruit harvested on October 12 from the Research Farm of Okayama University were used. Each point on days 0, 3, and 7 represents the mean value of four and three fruits, respectively. Vertical bars indicate \pm SE ($n = 3-4$). Statistical analysis was conducted by Tukey's multiple comparison test after one-way ANOVA. Different letters indicate significant differences among measurement days by Tukey's test ($p < 0.05$).

Supplementary Figure 3 | Amino acid sequence comparison of *PGM-M*⁰, *PGM-M*¹, and *PGF*. Amino acid sequences of *PGM-M*⁰, *PGM-M*¹, and *PGF* of peach and *PGM/F* of almond "Texas" (PdTX), "Lauranne" (PdLN), *P. kansuensis* (Pkan), apricot (Parm), Japanese apricot (Pmum), sweet cherry (Pavi), and *P. x yedoensis* (Pyed) were aligned by CLC Genomics Workbench. Red and blue arrowheads denote amino acid substitution in *PGM-M*¹ and *PGF*, respectively. The C-terminal region of PdLN_PGF was truncated because of the frameshift at third exon. Only one *PGM/F* was found in reference genome of almond "Texas," but it could be orthologous to *PGF* of reference genome of "Lauranne." *PGFs* of "Texas" and "Lauranne" shared some amino acid substitutions that were not conserved in *PGM* of "Lauranne."

Supplementary Figure 4 | Schematic representation of *NADH* genes. We compared the gene structures of *NADH0-3*, *NADH0/2* of M^{2r1} , and *NADH3/1* of M^{2b} . Boxes are exons. Gray exons are gene-specific sequences. Other region sequences are homologous to other genes. Sequence comparison with

Arabidopsis *NADH* indicated that the original *NADH* could be composed of five exons as shown in *NADH3/1* of M^{2b} and *NADH* of Japanese apricot (**Supplementary Figures S5, S6**).

Supplementary Figure 5 | Amino acid sequence comparison of *NADH*. Putative amino acid sequences of peach *NADHs* and Arabidopsis *NADH* (AtNADH; AT3G03080) were aligned by CLC Genomics Workbench.

Supplementary Figure 6 | Comparison of *NADH* gene structures among *Prunus* species. Gene structures of 11 *NADHs* from eight *Prunus* species were compared. Considering exon composition, *NADH3* and *NADH2* of peach were regarded as one gene (*NADH3/2*), although they were annotated as different genes in reference genome. *Pkan NADH* gene was divided into different contigs whose linkages were unknown. Disrupted structures were found in five *NADHs*: *Pkan_NADH*, *NADH3/2*, *Parm_NADH*, *PdLN_NADH3/2*, and *PdTX_NADH*. The others were intact structures. The M1 insertion was found at third intron of *NADH3/2* and *Parm_NADH*.

Supplementary Figure 7 | Nucleotide sequence comparison of *PGM-M⁰* and *-M^{0b}*. Sequence comparison showed six mutations in *PGM* of TH (designated as *PGM-M^{0b}* in this figure). Furthermore, a large insertion was predicted at the upstream region of *PGM-M^{0b}*. Of the six mutations, only one was located in CDS region and it was a synonymous substitution. AAC and AAT at 346–348 encode Asn. Therefore, we did not discriminate *PGM-M⁰* and *PGM-M^{0b}* in this study. In the study of Morgutti et al. (2017), *PGM-M^{0b}* was detected by CAPS analysis using *BstXI*. This restriction enzyme site was caused by the nucleotide substitution at 348 bp of *M^{0b}* haplotype and the fragment from *PGM-M⁰* was expected to be insensitive to *BstXI*. *PGM-M^{0b}* could confer the MF phenotype because flesh texture was melting in both TH ($M^{0b}M^3$) and BT ($M^{0b}M^3$). Morgutti et al. (2017) proposed four alleles, *PG_M*, *PG^m*, *PG^{SH}*, and *PG^{BT}*, at *M* locus from OA (M^2M^2), “Bolero” (M^1M^1), “Yumyeong” (M^0M^0), “Ghiaccio” (M^0M^0), and BT ($M^{0b}M^{03}$). Based on **Figure 7**, our classification suggested that *PG_M* and *PG^m* were derived from M^1 or M^2 haplotype and these were designated as *PGM-M¹* and *PGF*, respectively, in this study (**Supplementary Table S7**). *PG^{SH}* and *PG^{BT}* could correspond to *PGM-M⁰* and *PGM-M^{0b}*, respectively. These might be strictly different alleles because of the nucleotide substitution, but flesh texture was melting in both SM (M^0M^3) and TH ($M^{0b}M^3$), suggesting that their effects on flesh texture were the same and they were not different functionally.

Supplementary Figure 8 | Primers for PCR genotyping. Three primer sets were designed for the discrimination of four main haplotypes, M^0 , M^1 , M^2 , and M^3 . **(A)** Primer position at M^1 haplotype. **(B)** Position of *PGM/F* primer set.

Supplementary Figure 9 | MZ and O3 possessed M^{2b} haplotype. MZ and O3 possessed *PGM-M¹* and no *PGF*. This pattern indicated the M^2 haplotype, but no amplification to detect the M^2 deletion was observed by PCR (**Figure 8**). In addition to M^2 haplotype, we found the same combination in M^{2b} and M^{2r1} haplotypes, which were rare haplotypes compared with M^2 . To determine the genotypes of MZ and O3, we designed three primer sets to discriminate M^2 , M^{2b} , and M^{2r1} haplotypes on the basis of the sequences of *NADH* genes (**Supplementary Figure S4**). M2D2 amplified one fragment from M^0 , M^{2b} or M^{2r1} haplotype. NDP1 was expected to amplify two fragments: upper for M^0 , and lower for M^1 , M^2 , M^{2b} or M^{2r1} . NDP2 was also expected to amplify two fragments: upper for M^1 or M^{2b} , and lower for M^0 or M^{2r1} . The amplification of M2D2 fragment indicated MZ had M^0 , M^{2b} or M^{2r1} but not M^1 and M^2 . The lower NDP1 fragment in MZ excluded the possibility of M^0 . Furthermore, the upper NDP2 fragment was amplified in PCR, indicating that MZ possessed M^{2b} haplotype. O3 also had M^{2b} , but two fragments were amplified in NDP1 and NDP2 because O3 had M^0 haplotype (**Figure 8**).

Supplementary Figure 10 | Peach cultivars bred in Japan shared M^0 haplotype. HT, Hakuto; HH, Hakuho; AK, Akatsuki; BH, Benihakuto; YZ, Yuzora; TS, Tosui; KN, KawanakajimaHakuto; OB, Okubo; SM, ShimizuHakuto; O3, Okayama-3; HK, HikawaHakuho; LL, Lovell; CC, Chinese Cling (Shanghai Suimitsuto); TW,

Tachibanawase; UNK, unknown cultivar. **(A)** Genealogy of peach cultivars in Japan. Green cultivars were the five leading cultivars in Japan in 2016 (e-stat Japan, <https://www.e-stat.go.jp/>). Their cultivation areas accounted for more than 60% of the total peach cultivation area in Japan. Haplotypes in parentheses were presumed from haplotypes of offspring and another parent. **(B)** PCR haplotyping. CC was imported from China to Japan in the late nineteenth century. HT was reported to be found and selected as a chance seedling of CC in 1899 (Yamamoto et al., 2003a). HT was frequently used as seed parent in breeding programs and many Japanese peach cultivars were the progeny of HT, as described **Supplementary Figure S10A**. We selected 11 Japanese MF cultivars and carried out PCR genotyping to determine the genotypes of their *M* loci. All cultivars shared M^0 haplotype and all cultivars except OB and SM were M^0 homozygous. OB was M^0M^1 and SM was M^0M^3 . SM was found as a chance seedling at a mixed orchard of HT and O3. SSR analysis supported the hypothesis that SM was a progeny of HT (Yamamoto et al., 2003a). Because of male sterility of HT, O3 had been regarded as the pollen parent of SM. M^0 haplotype of SM was inherited from HT and seed parent should possess M^3 haplotype, because HT was M^0 homozygous. These indicated that O3 was not the parent of SM.

Supplementary Figure 11 | Structural comparison of *M* loci among *Prunus* species. Circos plots show sequence similarities among M^0 , M^1 , and *M* haplotypes of other *Prunus* species. Ribbons link homologous regions between haplotypes. *Indicates genes that did not have intact CDS sequence. *PG1* of *P. mume* was translocated to the > 2 Mbp downstream region. To determine the *M* locus region, reference genomes of almond (“Lauranne” and “Texas”), *P. kansuensis*, *P. mira*, Japanese apricot, apricot, sweet cherry, and *P. x yedoensis* were searched by Blastn analysis using *PG1*, *PG2*, *PGM/F*, *NADH*, and *F-box* genes as query. *M* locus was found at the right arm of chromosome 4 or LG3 in all *Prunus* species except *P. kansuensis*, in which no pseudomolecule was released. Nucleotide sequences of *M* locus were compared by nucmer and the relationships were drawn by Circos.

Supplementary Table 1 | Climate conditions in peach production areas in Okayama and Fukushima Prefectures, Japan in 2018.

Supplementary Table 2 | Relationships between flesh penetration force measured by the system used in this study and other fruit maturity indexes.

Supplementary Table 3 | Primers used in this study.

Supplementary Table 4 | Comparison of SNP number in regions from *PG1* to *PG2*. Intergenic region 1 was from end of *PG1* to 19,026,185 bp (outside M^3 deletion region). Intergenic region 2 was from 19,026,186 bp (inside M^3 deletion region) to start of *PG2*. Values in parentheses are those of heterozygous SNPs.

Supplementary Table 5 | *M* genotypes of 412 peach accessions.

Supplementary Table 6 | Differences in flesh texture predicted by genotype and reported phenotype. *The reported phenotype matched the predicted one in this study. The 11 accessions showed differences between predicted and reported phenotypes. All except “Early Gold” (EG) were reported by Yoon et al. (2006) and Cao et al. (2016). EG was a canning peach and its parent was “Nishiki” (NK). EG should possess at least one M^2 haplotype because NK was an M^2 homozygote, but resequencing analysis showed that EG was M^1M^1 .

Supplementary Table 7 | Correlation of *PGM/F* genes in this study with those in previous reports. *PG^{BT}* in Morgutti et al. (2017) was *BstXI*-sensitive (**Supplementary Figure S6**).

Supplementary Table 8 | Correlation of haplotypes in this study with those in previous reports. M^0 was misidentified as H_2 haplotype in Gu et al. (2016). *f* haplotype structure in Morgutti et al. (2017) was postulated from M^1 haplotype. *PG* gene composition was correct but the genome structure was not the same as M^0 haplotype in this study. *PGM-M⁰* and *PGM-M¹* were allelic.

REFERENCES

Bailey, J. S., and French, H. P. (1949). The inheritance of certain fruit and foliage characters in peach. *Mass. Agr. Expt. Sta. Bul.* 452, 2–31.

Bassi, D., and Monet, R. (2008). “Botany and taxonomy,” in *The Peach: Botany, Production and Uses*, eds D. R. Layne and D. Bassi (Wallingford: CAB International), 1–36. doi: 10.1079/9781845933869.0001

- Biale, J. B., and Young, R. E. (1981). "Respiration and ripening in fruits- retrospect and prospect," in *Recent Advances in the Biochemistry of Fruits and Vegetables*, eds J. Friend and M. J. C. Rhodes (London: Academic Press), 1–39. doi: 10.4324/9781315130590-1
- Brecht, J. K., and Kader, A. A. (1984). Ethylene production by fruit of some slow-ripening nectarine genotypes. *J. Am. Soc. Hort. Sci.* 109, 763–767.
- Brummell, D. A., Dal Cin, V., Crisosto, C. H., and Labavitch, J. M. (2004). Cell wall metabolism during maturation, ripening and senescence of peach fruit. *J. Exp. Bot.* 55, 2029–2039. doi: 10.1093/jxb/erh227
- Burg, S. P., and Burg, E. A. (1967). Molecular requirements for the biological activity of ethylene. *Plant Physiol.* 42, 144–152. doi: 10.1104/pp.42.1.144
- Callahan, A. M., Scorza, R., Bassett, C., Nickerson, M., and Abeles, F. B. (2004). Deletions in an endopolygalacturonase gene cluster correlate with non-melting flesh texture in peach. *Funct. Plant Biol.* 31, 159–168. doi: 10.1071/FP03131
- Cao, K., Zhou, Z., Wang, Q., Guo, J., Zhao, P., Zhu, G., et al. (2016). Genome-wide association study of 12 agronomic traits in peach. *Nat. Commun.* 7:13246. doi: 10.1038/ncomms13246
- Carrasco-Valenzuela, T., Muñoz-Espinoza, C., Riveros, A., Pedreschi, R., Arús, P., Campos-Vargas, R., et al. (2019). Expression QTL (eQTLs) analyses reveal candidate genes associated with fruit flesh softening rate in peach [*Prunus persica* (L.) Batsch]. *Front. Plant Sci.* 10:1581. doi: 10.3389/fpls.2019.01581
- Chin, S. W., Shaw, J., Haberle, R., Wen, J., and Potter, D. (2014). Diversification of almonds, peaches, plums and cherries—molecular systematics and biogeographic history of *Prunus* (Rosaceae). *Mol. Phylogenet. Evol.* 76, 34–48. doi: 10.1016/j.ympev.2014.02.024
- Clark, J. R., and Finn, C. E. (2010). Register of new fruit and nut cultivars List 45. *HortScience* 45, 716–756. doi: 10.21273/HORTSCI.45.5.716
- Davis, L. (1937). The gumming of Phillips cling peaches. *Hilgardia* 11, 1–34. doi: 10.3733/hilg.v11n01p001
- Eduardo, I., Picañol, R., Rojas, E., Batlle, I., Howad, W., Aranzana, M. J., et al. (2015). Mapping of a major gene for the slow ripening character in peach: co-location with the maturity date gene and development of a candidate gene-based diagnostic marker for its selection. *Euphytica* 205, 627–636. doi: 10.1007/s10681-015-1445-9
- Elsadr, H., Sherif, S., Banks, T., Somers, D., and Jayasankar, S. (2019). Refining the genomic region containing a major locus controlling fruit maturity in peach. *Sci. Rep.* 9:7522. doi: 10.1038/s41598-019-44042-4
- Fernandez, I., Marti, A., Sasaki, C. A., Manganaris, G. A., Gasic, K., and Crisosto, C. H. (2018). Genomic sequencing of Japanese plum (*Prunus salicina* Lindl.) mutants provides a new model for *Rosaceae* fruit ripening studies. *Front. Plant Sci.* 9:21. doi: 10.3389/fpls.2018.00021
- Fishman, M. L., Levaj, B., Gillespie, D., and Scorza, R. (1993). Changes in the physicochemical properties of peach fruit pectin during on-tree ripening and storage. *J. Amer. Soc. Hort. Sci.* 118, 343–349. doi: 10.21273/JASHS.118.3.343
- Font i Forcada, C., Oraguzie, N., Igartua, E., Ángele Moreno, M., and Gogorcena, Y. (2013). Population structure and marker-trait associations for pomological traits in peach and nectarine cultivars. *Tree Genet. Genomes* 9, 331–349. doi: 10.1007/s11295-012-0553-0
- Gapper, N. E., McQuinn, R. P., and Giovannoni, J. J. (2013). Molecular and genetic regulation of fruit ripening. *Plant Mol. Biol.* 82, 575–591. doi: 10.1007/s11103-013-0050-3
- Ghiani, A., Negrini, N., Morgutti, S., Baldin, F., Nocito, F. F., Spinardi, A., et al. (2011). Melting of "Big Top" nectarine fruit: some physiological, biochemical, and molecular aspects. *J. Am. Soc. Hort. Sci.* 136, 61–68. doi: 10.21273/JASHS.136.1.61
- Giné-Bordonaba, J., Eduardo, I., Arús, P., and Cantín, C. M. (2020). Biochemical and genetic implications of the slow ripening phenotype in peach fruit. *Sci. Hortic.* 259:108824. doi: 10.1016/j.scienta.2019.108824
- Gu, C., Wang, L., Wang, W., Zhou, H., Ma, B. Q., Zheng, H. Y., et al. (2016). Copy number variation of a gene cluster encoding endopolygalacturonase mediates flesh texture and stone adhesion in peach. *J. Exp. Bot.* 67, 1993–2005. doi: 10.1093/jxb/erw021
- Haji, T., Yaegaki, H., and Yamaguchi, M. (2003). Softening of stony hard peach by ethylene and the induction of endogenous ethylene by 1-aminocyclopropene-1-carboxylic acid (ACC). *J. Japan Soc. Hort. Sci.* 72, 212–217. doi: 10.2503/jjshs.72.212
- Haji, T., Yaegaki, H., and Yamaguchi, M. (2005). Inheritance and expression of fruit texture melting, non-melting and stony hard in peach. *Sci. Hortic.* 105, 241–248. doi: 10.1016/j.scienta.2005.01.017
- Hayama, H., Shimada, T., Fujii, H., Ito, A., and Kashimura, Y. (2006). Ethylene-regulation of fruit softening and softening-related genes in peach. *J. Exp. Bot.* 57, 4071–4077. doi: 10.1093/jxb/erl178
- Hayama, H., Tatsuki, M., and Nakamura, Y. (2008). Combined treatment of aminoethoxyvinylglycine (AVG) and 1-methylcyclopropene (1-MCP) reduces melting-flesh peach fruit softening. *Postharvest Biol. Technol.* 50, 228–230. doi: 10.1016/j.postharvbio.2008.05.003
- Hiwasa, K., Nakano, R., Hashimoto, A., Matsuzaki, M., Murayama, H., Inaba, A., et al. (2004). European, Chinese and Japanese pear fruits exhibit differential softening characteristics during ripening. *J. Exp. Bot.* 55, 2281–2290. doi: 10.1093/jxb/erh250
- Infante, R., Contador, L., Rubio, P., Aros, D., and Penja-Neira, A. i (2011). Postharvest sensory and phenolic characterization of 'Elegant Lady' and 'Carson' peaches. *Chilean J. Agric. Res.* 71, 445–451. doi: 10.4067/S0718-58392011000300016
- Jackman, S. D., Vandervalk, B. P., Mohamadi, H., Chu, J., Yeo, S., Hammond, S. A., et al. (2017). ABySS 2.0: resource-efficient assembly of large genomes using a Bloom filter. *Genome Res.* 27, 768–777. doi: 10.1101/gr.214346.116
- Kawai, T., Matsumori, F., Akimoto, H., Sakurai, N., Hirano, K., Nakano, R., et al. (2018). Nondestructive detection of split-pit peach fruit on trees with an acoustic vibration method. *Hort. J.* 87, 499–507. doi: 10.2503/hortj.UTD-012
- Kurtz, S., Phillippy, A., Delcher, A. L., Smoot, M., Shumway, M., Antonescu, C., et al. (2004). Versatile and open software for comparing large genomes. *Genome Biol.* 5:R12. doi: 10.1186/gb-2004-5-2-r12
- Lester, D. R., Sherman, W. B., and Atwell, B. J. (1996). Endopolygalacturonase and the melting flesh (M) locus in peach. *J. Amer. Soc. Hort. Sci.* 121, 231–235. doi: 10.21273/JASHS.121.2.231
- Lester, D. R., Speirs, G., Orr, G., and Brady, C. J. (1994). Peach (*Prunus persica*) endo-PG cDNA isolation and mRNA analysis in melting and non-melting peach cultivars. *Plant Physiol.* 105, 225–231. doi: 10.1104/pp.105.1.225
- Li, H. (2018). Minimap2: pairwise alignment for nucleotide sequences. *Bioinformatics* 34, 3094–3100. doi: 10.1093/bioinformatics/bty191
- Liguori, G., Weksler, A., Zutahi, Y., Lurie, S., and Kosto, I. (2004). Effect of 1-methylcyclopropene on ripening of melting flesh peaches and nectarines. *Postharvest Biol. Technol.* 31, 263–268. doi: 10.1016/j.postharvbio.2003.09.007
- Liu, H., Qian, M., Song, C., Li, J., Zhao, C., Li, G., et al. (2018). Down-regulation of *PpBGAL10* and *PpBGAL16* delays fruit softening in peach by reducing polygalacturonase and pectin methylesterase activity. *Front. Plant Sci.* 9:1015. doi: 10.3389/fpls.2018.01015
- Mathooko, F. M., Tsunashima, Y., Owino, W. Z. O., Kubo, Y., and Inaba, A. (2001). Regulation of genes encoding ethylene biosynthetic enzymes in peach (*Prunus persica* L.) fruit by carbon dioxide and 1-methylcyclopropene. *Postharvest Biol. Technol.* 21, 265–281. doi: 10.1016/S0925-5214(00)00158-7
- McMurchie, E. J., McGlasson, W. B., and Eaks, I. L. (1972). Treatment of fruit with propylene gives information about bio-genesis of ethylene. *Nature* 237, 235–236. doi: 10.1038/237235a0
- Meneses, C., Ulloa-Zepeda, L., Cifuentes-Esquivel, A., Infante, R., Cantin, C. M., Batlle, I., et al. (2016). A codominant diagnostic marker for the slow ripening trait in peach. *Mol. Breed.* 36:77. doi: 10.1007/s11032-016-0506-7
- Minas, I. S., Font i Forcada, C., Dangl, G. S., Gradziel, T., Dandekar, A. M., and Crisosto, C. H. (2015). Discovery of non-climacteric and suppressed-climacteric bud sport mutations originating from a climacteric Japanese plum cultivar (*Prunus salicina* lindl.). *Front. Plant Sci.* 6:316. doi: 10.3389/fpls.2015.00316
- Moggia, C., Graell, J., Lara, I., González, G., and Lobos, G. A. (2017). Firmness at harvest impacts postharvest fruit softening and internal browning development in mechanically damaged and non-damaged highbush blueberries (*Vaccinium corymbosum* L.). *Front. Plant Sci.* 8:535. doi: 10.3389/fpls.2017.00535
- Monet, R. (1989). Peach genetics: past, present and future. *Acta Hortic.* 254, 49–57. doi: 10.17660/ActaHortic.1989.254.8
- Morgutti, S., Negrini, N., Ghiani, A., Baldin, F., Bassi, D., and Cocucci, M. (2017). Endopolygalacturonase gene polymorphisms: asset of the locus in different peach accessions. *Am. J. Plant Sci.* 8, 941–957. doi: 10.4236/ajps.2017.84063
- Morgutti, S., Negrini, N., Nocito, F. F., Ghiani, A., Bassi, D., and Cocucci, M. (2006). Changes in endopolygalacturonase levels and characterization of

- a putative *endo-PG* gene during fruit softening in peach genotypes with nonmelting and melting flesh fruit phenotypes. *New Phytol.* 171, 315–328. doi: 10.1111/j.1469-8137.2006.01763.x
- Nakano, R., Akimoto, H., Fukuda, F., Kawai, T., Ushijima, K., Fukamatsu, Y., et al. (2018). Nondestructive detection of split pit in peaches using an acoustic vibration method. *Hort. J.* 87, 281–287. doi: 10.2503/hortj.OKD-094
- Nimmakayala, P., Tomason, Y. R., Abburi, V. L., Alvarado, A., Saminathan, T., Vajja, V. G., et al. (2016). Genome-wide differentiation of various melon horticultural groups for use in GWAS for fruit firmness and construction of a high resolution genetic map. *Front. Plant Sci.* 7:1437. doi: 10.3389/fpls.2016.01437
- Nishiyama, K., Guis, M., Rose, J. K., Kubo, Y., Bennett, K. A., Wangjin, L., et al. (2007). Ethylene regulation of fruit softening and cell wall disassembly in *Charentais* melon. *J. Exp. Bot.* 58, 1281–1290. doi: 10.1093/jxb/erl283
- Núñez-Lillo, G., Cifuentes-Esquivel, A., Troggo, M., Micheletti, D., Infante, R., Campos-Vargas, R., et al. (2015). Identification of candidate genes associated with mealiness and maturity date in peach [*Prunus persica* (L.) Batsch] using QTL analysis and deep sequencing. *Tree Genet. Genomes* 11:86. doi: 10.1007/s11295-015-0911-9
- Pan, L., Zeng, W., Niu, L., Lu, Z., Liu, H., Cui, G., et al. (2015). *PpYUC11*, a strong candidate gene for the stony hard phenotype in peach (*Prunus persica* L. Batsch), participates in IAA biosynthesis during fruit ripening. *J. Exp. Bot.* 66, 7031–7044. doi: 10.1093/jxb/erv400
- Peace, C. P., Callahan, A., Ogundiwin, E. A., Potter, D., Gradziel, T. M., Bliss, F. A., et al. (2007). Endopolygalacturonase genotypic variation in *Prunus*. *Acta Hort.* 738, 639–646. doi: 10.17660/actahortic.2007.738.83
- Peace, C. P., Crisosto, C. H., and Gradziel, T. M. (2005). Endopolygalacturonase: a candidate gene for freestone and melting flesh in peach. *Mol. Breed.* 16, 21–31. doi: 10.1007/s11032-005-0828-3
- Pressey, R., and Avants, J. K. (1978). Differences in polygalacturonase composition of clingstone and freestone peaches. *J. Food Sci.* 43, 1415–1423. doi: 10.1111/j.1365-2621.1978.tb02507.x
- Tatsuki, M., Haji, T., and Yamaguchi, M. (2006). The involvement of 1-aminocyclopropane-1-carboxylic acid synthase isogene, *Pp-ACS1*, in peach fruit softening. *J. Exp. Bot.* 57, 1281–1289. doi: 10.1093/jxb/erj097
- Tatsuki, M., Soeno, K., Shimada, Y., Sawamura, Y., Suesada, Y., Yaegaki, H., et al. (2018). Insertion of a transposon-like sequence in the 5'-flanking region of the *YUCCA* gene causes the stony hard phenotype. *Plant J.* 96, 815–827. doi: 10.1111/tpj.14070
- Tonutti, P., Casson, P., and Ramina, A. (1991). Ethylene biosynthesis during peach fruit development. *J. Amer. Soc. Hort. Sci.* 116, 274–279. doi: 10.21273/JASHS.116.2.274
- Tucker, G., Yin, X., Zhang, A., Wang, M., Zhu, Q., Liu, X., et al. (2017). Ethylene and fruit softening. *Food Qual. Safe* 1, 253–267. doi: 10.1093/fqsafe/fyx024
- Verde, I., Jenkins, J., Dondini, L., Micali, S., Pagliarani, G., Vendramin, E., et al. (2017). The Peach v2.0 release: high-resolution linkage mapping and deep resequencing improve chromosome-scale assembly and contiguity. *BMC Genomics* 18:225. doi: 10.1186/s12864-017-3606-9
- Wang, Z.-H., and Lu, Z.-X. (1992). Advances of peach breeding in China. *HortScience* 27, 729–732. doi: 10.21273/HORTSCI.27.7.729
- Yamamoto, T., Mochida, K., and Hayashi, T. (2003a). Shanhai suimitsuto, one of the origins of Japanese peach cultivars. *J. Japan. Soc. Hort. Sci.* 72, 116–121. doi: 10.2503/jjshs.72.116
- Yamamoto, T., Mochida, K., Imai, T., Haji, T., Yaegaki, H., Yamaguchi, M., et al. (2003b). Parentage analysis in Japanese peaches using SSR markers. *Breed. Sci.* 53, 35–40. doi: 10.1270/jsbbs.53.35
- Yamazaki, T., and Suzuki, K. (1980). Color charts: useful guide to evaluate the fruit maturation. I. Colorimetric specifications of color charts for Japanese pear, apple, peach, grape, kaki and citrus fruits. (In Japanese with English summary). *Bull. Fruit Tree Res. Sta.* A 19–44.
- Yoon, J., Liu, D., Song, W., Liu, W., Zhang, A., and Li, S. (2006). Genetic diversity and ecogeographical phylogenetic relationships among peach and nectarine cultivars based on simple sequence repeat (SSR) markers. *J. Am. Soc. Hort. Sci.* 131, 513–521. doi: 10.21273/JASHS.131.4.513
- Yoshida, M. (1981). Recent trend of peach breeding in Japan. *JARQ* 15, 106–109.
- Yoshioka, H., Hayama, H., Tatsuki, M., and Nakamura, Y. (2010). Cell wall modification during development of mealy texture in the stony-hard peach “Odoroki” treated with propylene. *Postharvest Biol. Technol.* 55, 1–7. doi: 10.1016/j.postharvbio.2009.08.005
- Yoshioka, H., Hayama, H., Tatsuki, M., and Nakamura, Y. (2011). Cell wall modifications during softening in melting type peach “Akatsuki” and non-melting type peach “Mochizuki”. *Postharvest Biol. Technol.* 60, 100–110. doi: 10.1016/j.postharvbio.2010.12.013
- Zhang, X., Su, M., Du, J., Zhou, H., Li, X., Li, X., et al. (2019). Comparison of phytochemical differences of the pulp of different peach [*Prunus persica* (L.) Batsch] cultivars with alpha-glucosidase inhibitory activity variations in China using UPLC-Q-TOF/MS. *Molecules* 24:1968. doi: 10.3390/molecules24101968

Conflict of Interest: The authors declare that the research was conducted in the absence of any commercial or financial relationships that could be construed as a potential conflict of interest.

Copyright © 2020 Nakano, Kawai, Fukamatsu, Akita, Watanabe, Asano, Takata, Sato, Fukuda and Ushijima. This is an open-access article distributed under the terms of the Creative Commons Attribution License (CC BY). The use, distribution or reproduction in other forums is permitted, provided the original author(s) and the copyright owner(s) are credited and that the original publication in this journal is cited, in accordance with accepted academic practice. No use, distribution or reproduction is permitted which does not comply with these terms.